

Jakob Philipp Ebner

Optical Properties of Semiconductor-Metal Hybrid Nanoparticles

Diplomarbeit

zur Erlangung des akademischen Grades eines
Magisters
an der Naturwissenschaftlichen Fakultät der
Karl-Franzens-Universität Graz



Betreuer: Ao. Univ. Prof. Mag. Dr. Ulrich Hohenester

Institut für Physik
Fachbereich Theoretische Physik

2013

Contents

1. Introduction	1
1.1. Prologue	1
1.2. Structure of this thesis	3
2. Basic Principles	4
2.1. Electromagnetic fields	4
2.1.1. Direct Coulomb interaction	4
2.1.2. Maxwell's equations	6
2.1.3. Quasistatic approximation	7
2.2. Plasmons	8
2.2.1. Dielectric function of metals	9
2.2.2. Surface Plasmons	10
2.2.3. Particle Plasmons	13
2.3. Semiconductors	14
2.3.1. Excitons	14
2.3.2. Effective Mass	15
2.3.3. Interband Polarization	16
2.4. Nano and Quantum optics	17
2.4.1. Dipole Approximation	18
2.4.2. Rotating Wave Approximation	18
2.4.3. Cross sections	19
3. Theory	22
3.1. Describing the System	22
3.2. Polarization	24
3.3. Optical response	26
4. Numerics	30
4.1. Discretizing the Hamiltonian	30
4.2. Boundary Element Method	30
4.2.1. BEM theory	31
4.2.2. Surface discretization	32
4.3. Program outline	33

Contents

5. Results	35
5.1. Combining Particles	36
5.2. Charge carrier densities	37
5.3. Polarization	39
5.4. Optical response	41
5.5. Influence of numerical parameters	43
5.5.1. Grid size	43
5.5.2. Number of states	44
5.6. Problems	44
5.7. Conclusion	44
Acknowledgements	46
A. Calculations	47
A.1. Boundary Conditions	47
A.2. Potentials in media	49
A.3. Exciton wave functions	51
B. Conventions and Conversions	53
B.1. Atomic Units	53
B.2. Gaussian-CGS Units	54
B.3. Energy conversion	54
Bibliography	56

Abstract

In this thesis I study the optical properties of a hybrid nanoparticle consisting of a metal and a semiconductor part. I examine the electrostatic influence of the metallic particle on the exciton states. Further, I calculate the effect of the semiconductor on the plasmon that is optically created on the metal surface. I derive a framework to calculate the polarization of the semiconductor due to the external and plasmonic fields, and use it to obtain the scattering and absorption spectra for the combined particle.

I treat a model system where the semiconductor is approximated by a few material specific parameters and the geometry is a match stick shaped structure with a semiconducting rod and a metallic tip. For our simulations I use the MNPBEM [1] toolbox for Matlab, which uses the boundary element method [2] for the calculation of electromagnetic potentials.

I find that the optical response of the combined particle is enhanced with respect to the response of separated particles. Exciton resonances are shifted to lower energies in the presence of a metal and the exciton-dipole self interaction via the environment appears to have very little effect on the optical properties.

1. Introduction

1.1. Prologue

Particles whose dimensions do not exceed the nanometer scale at least in one dimension are called *nanoparticles*. They live at the boundary of the quantum and the classical world, small enough to exhibit quantum mechanical behaviour but still consisting of thousands to millions of atoms. Since great progress has been made in manufacturing such small particles, many new effects can be studied and new applications can be found in this area.

A very interesting feature of metallic nanoparticles, that was even used in Roman times, is the occurrence of particle plasmons. These are oscillations of electrons in a metal that can be driven by an electromagnetic wave. They exhibit optical properties strongly depending on the size and geometry of the particles, and not only on the material, as common pigments do. The ancient example for particle plasmons mentioned above is the Lycurgus cup (Fig. 1.1) which appears to have different colors depending on the direction of illumination. It appears green if lighted from the front but looks red if illuminated from the back or from inside. This behaviour comes from different resonance properties of plasmons in light absorption and scattering. In the first case one sees the reflected light, and in the second case one sees the light after specific frequencies are absorbed. This technique, namely adding tiny portions of gold and silver nanoparticles to the glass, was also used in more “recent” history for colorful church windows where normal dyes would have dissolved long ago.

A very important feature for the application of plasmons is the occurrence of a very strong electric field at the metallic surface that can be several magnitudes stronger than the exciting light field. This so called *evanescent field* is strongly

1. Introduction



Figure 1.1.: Lycurgus cup at the British Museum in London. Different wavelengths are absorbed in reflection (left) and transmission (right).

localized and decays exponentially when moving away from the surface. The fact that plasmon resonances are very sensitive to the dielectric function of the surrounding medium makes them very interesting for sensor applications. Further possible applications of plasmonic structures are submicron optical waveguides for optoelectronics, medical treatments[3] and the use as catalysts because of their high surface to volume ratio.

Nanoparticles whose surfaces exhibit two or more distinct physical properties are called *Janus particles*. This can either be achieved by combining different materials or different surface treatments of distinct parts of the particle. The progress in synthesis has not only made it possible to shape one material at an ever smaller scale, but also to combine different materials at the nanoscale. This gives the opportunity to directly combine the promising properties of metallic nanoparticles with the widely used properties of semiconductors.

The purpose of this thesis is to study and simulate the optical properties of such a hybrid semiconductor metal particle. In this case we have to consider not only that the enhanced field of the metallic particle does influence the charge carrier response inside the semiconductor but also that a plasmon is very sensitive to changes in the dielectric environment and therefore its properties also depend on the size and shape of the semiconductor attached to the metallic nanoparticle.

1. Introduction

In particular, we are interested in the influence of the exciton excitations on the optical properties of the system. In this thesis we treat a matchstick shaped structure consisting of a semiconductor nanorod with an attached gold sphere, which is dissolved in toluene, as an example for such a system.

1.2. Structure of this thesis

After this introduction we summarize some textbook knowledge that is necessary for our further investigations in chapter 2. Chapter 3 will show our theoretical approach to the systems Hamiltonian and the optical response. In chapter 4 we translate our findings of chapter 3 into a numerical scheme. Our final results will be presented in chapter 5 where we will compare the behaviour of the combined particles to its components and show its scattering and absorption cross sections. Some auxiliary calculations can be found in Appendix A.

Throughout the theory part we use Hartree atomic units and CGS units (Appendix B). The results are presented in milli-electron Volts (meV) and nanometers (nm). Operators are not emphasized explicitly but should be recognizable as such.

2. Basic Principles

In this chapter we will gather some textbook results of the topics that are crucial for the understanding of this thesis. Most of them will only be touched briefly, but further references will be given in each section.

2.1. Electromagnetic fields

In this section we will give a short overview of some aspects of classical electrodynamics following references [4] and [5]. We remind you that all formulas will be in the cgs unit system.

2.1.1. Direct Coulomb interaction

Electrostatics is based on Coulomb's law, which was discovered in the second half of the 18th century and first published by Charles Auguste de Coulomb [6]. It describes the vectorial force of an arbitrary charge distribution $\rho(\mathbf{r}')$ on a charge q at position \mathbf{r} in vacuum

$$\mathbf{F} = q \int \rho(\mathbf{r}') \frac{(\mathbf{r} - \mathbf{r}')}{|\mathbf{r} - \mathbf{r}'|^3} d\tau'. \quad (2.1)$$

The concept to describe electrostatics and electrodynamics in modern physics, is with fields and potentials

$$\Phi(r) = \int \frac{\rho(\mathbf{r}')}{|\mathbf{r} - \mathbf{r}'|} d\tau'. \quad (2.2)$$

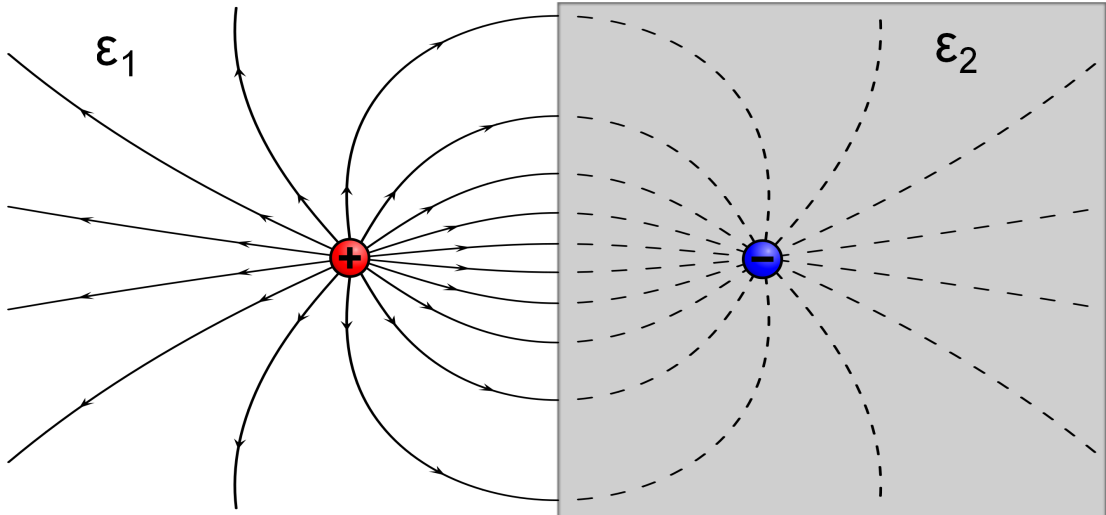


Figure 2.1.: The potential of a charge in medium 1 near a flat surface of medium 2 can be described as the potential of two charges in medium 1. The position of the second charge is just the inversion of position 1 with respect to the surface. The charge depends on the material, it is exactly opposite to the original charge if medium 2 is a metal.

Usually in solids the charge densities of the negative electrons and positive cores cancel each other out, at least if one does not look too closely. But if we look at a solid with an additional free charge present, the situation differs. The positive and negative charges in the solid react differently on the additional potential generating an effective charge density inside the material. This creates a potential which acts back on the free charge, leading to an effective self interaction of free charges in the presence of media. In the hypothetical case where we consider the medium to fill a half space, the induced potential is identical to the potential of another charge situated exactly symmetric with respect to the solid surface (Fig. 2.1). This example coins the term *image charge* for this effect. A detailed analysis of self interaction in more complex geometries can be found in [7]. This effect will play an important role for the charges confined in the semiconductor part of our hybrid matchstick.

2.1.2. Maxwell's equations

Between 1861 and 1865 Clark Maxwell cast the whole knowledge about electrodynamics in dielectric media into the four following equations [8]

$$\nabla \cdot \mathbf{D}(\mathbf{r}, t) = 4\pi\rho(\mathbf{r}, t), \quad (2.3a)$$

$$\nabla \cdot \mathbf{B}(\mathbf{r}, t) = 0, \quad (2.3b)$$

$$\nabla \times \mathbf{H}(\mathbf{r}, t) = \frac{4\pi}{c}\mathbf{j}(\mathbf{r}, t) + \frac{1}{c}\frac{\partial \mathbf{D}(\mathbf{r}, t)}{\partial t}, \quad (2.3c)$$

$$\nabla \times \mathbf{E}(\mathbf{r}, t) = -\frac{1}{c}\frac{\partial \mathbf{B}(\mathbf{r}, t)}{\partial t}. \quad (2.3d)$$

Where \mathbf{D} is the dielectric displacement, \mathbf{E} the electric field, \mathbf{B} and \mathbf{H} are the magnetic induction and magnetic field and ρ and \mathbf{j} are the free charge and current densities. In isotropic linear media the dielectric displacement simply reads $\mathbf{D} = \varepsilon \mathbf{E}$ and the magnetic fields are related via $\mathbf{B} = \mu \mathbf{H}$. ε is the permittivity which we assume constant in space, for each medium, throughout this thesis. μ is the magnetic permeability which can be set to one at optical frequencies.

From these four equations we deduce that the electric and magnetic fields are not independent. Indeed they can be rewritten in form of the scalar potential ϕ and the magnetic vector potential \mathbf{A} as

$$\mathbf{E} = -\nabla\phi - \frac{1}{c}\frac{\partial}{\partial t}\mathbf{A}, \quad \mathbf{B} = \nabla \times \mathbf{A}. \quad (2.4)$$

One can easily see that the potentials automatically fulfill the homogeneous Maxwell equations (2.3b) and (2.3d). But these definitions do not uniquely define the potentials and leave a so called *freedom of gauge*. To reduce these redundancies one can introduce conditions on the potentials that may simplify the problem at hand. We want to derive wave equations for the potentials and therefore introduce the Lorentz condition

2. Basic Principles

$$\nabla \cdot \mathbf{A} + \epsilon \frac{1}{c} \frac{\partial}{\partial t} \phi = 0. \quad (2.5)$$

If we consider harmonic electromagnetic waves with a time dependence $e^{-i\omega t}$ and the wave vector $k = \omega/c$ the time derivative simplifies to $\partial/\partial t = -i\omega$ and we can deduce from (2.3a)

$$\nabla \cdot \mathbf{E} = \nabla \cdot (-\nabla\phi + ik\mathbf{A}) = -\nabla^2\phi + ik\nabla\mathbf{A} = 4\pi\frac{\rho}{\epsilon}. \quad (2.6)$$

In combination with the Lorenz condition this gives

$$\nabla^2\phi + k^2\epsilon\phi = -4\pi\frac{\rho}{\epsilon}. \quad (2.7)$$

By starting from (2.3c) we can analogously derive a similar equation for the vector potential

$$\nabla^2\mathbf{A} + k^2\epsilon\mathbf{A} = -\frac{4\pi}{c}\mathbf{j}. \quad (2.8)$$

These equations are called the *Helmholtz equations* for potentials and are equivalent to Maxwell's equations.

2.1.3. Quasistatic approximation

If we examine a particle much smaller than the light wavelength we can neglect retardation effects and assume the electromagnetic field constant throughout the particle. Thus, we set $k \approx 0$ which leads to a vanishing vector potential \mathbf{A} in Lorentz gauge (2.5) and the Helmholtz equation of the scalar potential (2.7) simplifies to the *Poisson equation*

$$\nabla^2\Phi = -4\pi\frac{\rho}{\epsilon}. \quad (2.9)$$

For the homogeneous case, in which no free charges are present, this results in the *Laplace equation*

2. Basic Principles

$$\nabla^2\phi = 0. \tag{2.10}$$

For the solution of the Poisson equation we can employ the *Green's function* formalism. Green's functions are a well established tool to solve inhomogeneous differential equations. The inhomogeneous part of a differential equation can be solved with the help of such a Green's function which is defined as a solution of

$$\hat{D} G(\mathbf{r}, \mathbf{r}') = -4\pi\delta(\mathbf{r}, \mathbf{r}'). \tag{2.11}$$

For the Poisson equation, $\hat{D} = \nabla^2$, in a homogeneous unbound medium there exists a relatively simple solution to this problem. The so-called electrostatic Green's function

$$G(\mathbf{r}, \mathbf{r}') = \frac{1}{\epsilon|\mathbf{r} - \mathbf{r}'|}, \tag{2.12}$$

where the factor $1/\epsilon$, which appears on the right hand side of (2.9), is already incorporated into the Green's function. With this Green's function we can write the solution of the Poisson equation (2.9) as $\phi(\mathbf{r}) = \int G(\mathbf{r}, \mathbf{r}', \epsilon)\rho(\mathbf{r}')d\mathbf{r}'$ plus any function that satisfies the Laplace equation (2.10).

Thus, in homogeneous media where ϵ is constant inside the medium, we can transform the volume integral into a surface integral using Gauss's theorem and write the solution for the potential in the ad-hoc form [2, 9]

$$\phi(\mathbf{r}) = \phi_{ext}(\mathbf{r}) + \oint G(\mathbf{r}, \mathbf{s})\sigma(\mathbf{s})da. \tag{2.13}$$

2.2. Plasmons

Plasmons are the quasiparticles of quantized collective oscillations of the free electron gas in solids, similar to phonons, the quasiparticles of vibrations. They can be divided into bulk plasmons, surface plasmons and particle plasmons. Bulk plasmons, which are e.g. responsible for the shiny appearance of metals, are situated

2. Basic Principles

throughout the whole volume of a solid, surface plasmons are located at interfaces between a metal and a dielectric, and particle plasmons occur at metallic particles which are smaller than the light wavelength.

The topics treated in this section are discussed in more detail in [10] and [11].

2.2.1. Dielectric function of metals

A simple, but very effective, way to describe the response of a metal to an applied electric field is the Drude-Sommerfeld theory. The free electron gas is treated in a classical kinetic fashion, and a damped harmonic oscillator is obtained for the equation of motion

$$m \frac{\partial^2 \mathbf{r}}{\partial t^2} + m\gamma \frac{\partial \mathbf{r}}{\partial t} = e \mathbf{E}_0 e^{-i\omega t}, \quad (2.14)$$

where γ is a material specific damping term, m and e are the mass and charge of an electron respectively, \mathbf{E}_0 is the amplitude and ω the frequency of the external electric field. With the ansatz $\mathbf{r} = \mathbf{r}_0 e^{-i\omega t}$ we can derive the polarization of the metal and therefore get the dielectric function in Drude form

$$\epsilon(\omega) = 1 - \frac{\omega_p^2}{\omega^2 + i\gamma\omega}, \quad (2.15)$$

where ω_p is the *bulk plasma frequency* that depends on the electron density in the corresponding metal. If we assume a negligible damping we can conclude that the refractive index $n = \sqrt{\epsilon}$ becomes strictly imaginary and light can not penetrate the metal very far if the exciting frequency ω is smaller than ω_p .

What the formulas above do not take into account is that electrons can absorb the energy of the electric field to be excited into a higher band. This leads to a breakdown of the theory around and above the transition energies, for gold this is the case for wavelengths around 550 nm. There exist theoretical approaches to include these interband transitions [11], but in this thesis we use experimental values for the dielectric functions [12].

2.2.2. Surface Plasmons

In this section we will discuss plasmons located at an interface between a metal and a dielectric. We will derive the necessary requirements for the existence of such a plasmon. Therefore we will start by applying Maxwell's equations to such an interface.

We already know that the Helmholtz equation (2.7) follows directly from Maxwell's equations in a source free environment, and in terms of the dielectric function it looks like

$$\left(\nabla^2 + \epsilon(\mathbf{r}, \omega) \frac{\omega^2}{c^2} \right) \mathbf{E}(\mathbf{r}, \omega) = 0 \quad (2.16)$$

If we look at a flat interface perpendicular to the z -axis at $z=0$, we can describe the environment with the dielectric function

$$\epsilon(\mathbf{r}, \omega) = \begin{cases} \epsilon_1(\omega), & \text{if } z > 0, \\ \epsilon_2(\omega), & \text{if } z < 0, \end{cases} \quad (2.17)$$

with ϵ_1 being positive and therefore representing a dielectric, while ϵ_2 is negative and corresponds to the metal. If we split the electric field into a transversal electric (TE) and a transversal magnetic (TM) mode one can show that there is no solution to the Helmholtz equation in the TE case [11]. Therefore we will now take a closer look at the TM mode, where the electric fields in the media are

$$\mathbf{E}_j = E_{j,x} \begin{pmatrix} 1 \\ 0 \\ -k_x/k_{j,z} \end{pmatrix} e^{i(k_x x + k_{j,z} z - \omega t)}, \quad (2.18)$$

where j is the index to the respective medium. Because the parallel component of the wave vector is conserved at the interface, we get the condition

$$k_x^2 + k_{j,z}^2 = \epsilon_j k^2. \quad (2.19)$$

2. Basic Principles

Since we do not consider free charges in our current examination we find from (2.3a) that

$$k_x E_{j,x} + k_{j,z} E_{j,z} = 0. \quad (2.20)$$

Inserting this into (2.18) we arrive at

$$\mathbf{E}_j = E_{j,x} \begin{pmatrix} 1 \\ 0 \\ -k_x/k_{j,z} \end{pmatrix} e^{i(k_x x + k_{j,z} z - \omega t)}. \quad (2.21)$$

The surface plasmons also have to obey the boundary conditions for the electric field (section A.1):

$$\begin{aligned} E_{1,x} - E_{2,x} &= 0, \\ \epsilon_1 E_{1,z} - \epsilon_2 E_{2,z} &= 0. \end{aligned} \quad (2.22)$$

If we want to satisfy equations (2.20) and (2.22) we arrive at two alternatives. The first one is $k_x = 0$, where clearly no wave is propagating along the surface. The second possibility is

$$\epsilon_1 k_{2,z} - \epsilon_2 k_{1,z} = 0. \quad (2.23)$$

Together with (2.20) this yields the following dispersion relations

$$k_x^2 = \frac{\epsilon_1 \epsilon_2}{\epsilon_1 + \epsilon_2} k^2 = \frac{\epsilon_1 \epsilon_2}{\epsilon_1 + \epsilon_2} \frac{\omega^2}{c^2}, \quad (2.24)$$

$$k_{j,z}^2 = \frac{\epsilon_j^2}{\epsilon_1 + \epsilon_2} k^2. \quad (2.25)$$

Since we are interested in a propagating wave in x-direction we require a real k_x , which imposes certain relations on the dielectric functions. If we look at (2.24) we

2. Basic Principles

see that the product and the sum of the dielectric functions need to have the same sign. Furthermore, we demand an imaginary k_z because we want waves localized at the surface and not propagating into the media. This gives for the dielectric functions

$$\epsilon_1(\omega) \cdot \epsilon_2(\omega) < 0, \quad (2.26)$$

$$\epsilon_1(\omega) + \epsilon_2(\omega) < 0. \quad (2.27)$$

These relations are fulfilled if we combine a metal which has a negative dielectric function with a dielectric which usually has a positive dielectric function smaller than that of the metal.

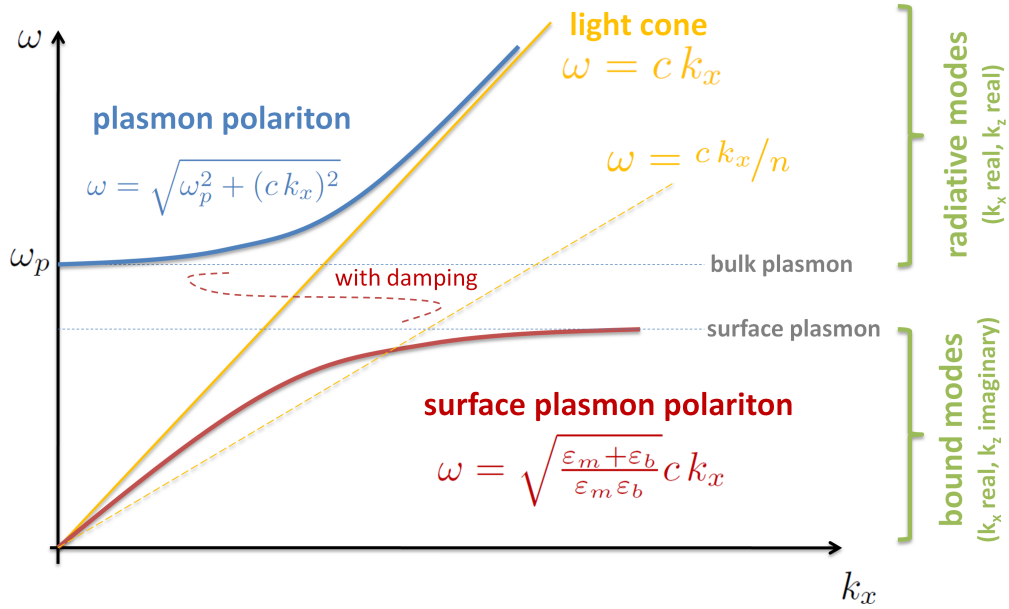


Figure 2.2.: Dispersion relation of a surface plasmon. Here we assume a surface between vacuum and metal. The dispersion relation of light in vacuum (yellow solid line) does not cross the dispersion relation of the surface plasmon (red). An incoming wave in the dielectric (yellow dashed) crosses the red line and a surface plasmon with this frequency can be excited (source: [13]).

In Fig. 2.2 the dispersion relation of the surface plasmon is plotted together with that of light in the dielectric $\omega = k_x c/n_d$. We see that no surface plasmon can be excited by such an electromagnetic wave because the lines of the dispersion relations do not cross, which means, that energy-momentum conservation can not

2. Basic Principles

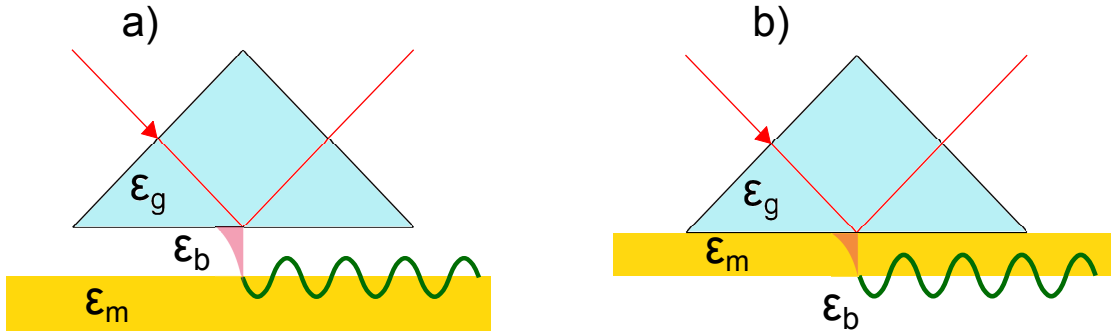


Figure 2.3.: Excitation of surface plasmon. If the dielectric of the prism is higher than that of the background total can occur and the dispersion in the prism is less steep than in the background. The evanescent field of the totally reflected wave in the prism has the same dispersion relation as the wave itself, therefore it can excite a surface plasmon at the interface between background and metal. For a) the Otto geometry it is difficult to keep the distance constant whereas for b) the Kretschmann-Raether geometry the thickness of the metal film has to be smaller than the skin depth of the evanescent field.

be fulfilled. A solution to achieve such an excitation is to “tilt” the light line by slowing down the exciting light. This means that the light has to come in through an optically thicker medium than the dielectric along which the surface plasmon propagates. This can be accomplished in the Kretschmann-Raether geometry [14] or the Otto geometry [15] which are shown in Fig. 2.3.

2.2.3. Particle Plasmons

If we turn from a planar interface to a metallic nanoparticle that is smaller than the exciting wavelength we do not have propagating waves but localized plasmons. The free electron gas in the metal gets polarized and the ionic background exhibits a restoring force. Thus the particle acts as an oscillator whose resonance not only depends on the properties of the involved media but is also strongly influenced by the geometry and size of the particle.

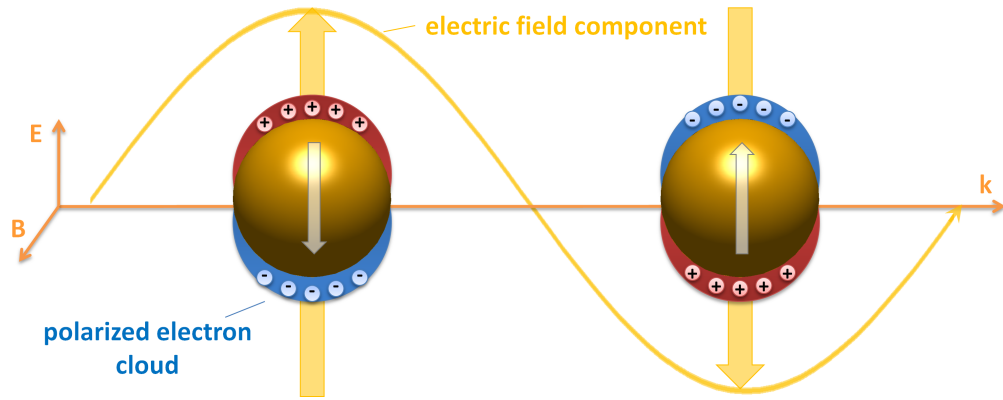


Figure 2.4.: Particle plasmon. The whole particle gets polarized by the electromagnetic wave (source: [13]).

2.3. Semiconductors

Semiconductors are shaping our everyday lives because most of our electronic devices contain a computer chip which can only work because of the special properties of semiconductors. But not just their electric transport properties make them interesting, they also have unique optical properties. Semiconductors in the ground state would behave like an insulator but the low energy gap between the valence band filled with electrons and the empty conduction band makes it relatively easy to optically excite electrons into the conduction band.

The electrical properties can be described by intraband transitions, carrier-carrier interactions inside the respective bands. But we are interested in the optical properties which are connected to interband transitions, processes that change the band of an electron. One way to achieve an excitation of an electron into the conduction band is to shine light, that matches the energy difference between the bands, onto the semiconductor. The bandgap of many semiconductors is in the visible or near infrared light regime.

We will now derive some of the optical properties of semiconductors following [16].

2.3.1. Excitons

If a bound electron gets excited it leaves behind a positively charged *hole*. These two different charge carriers will then be coupled by an attractive Coulomb force.

2. Basic Principles

This can be described quantum mechanically through a quasiparticle called *exciton*. We can distinguish two limiting cases - strongly bound Frenkel excitons and loosely bound Wannier or Wannier-Mott excitons. Frenkel excitons are created in materials where the Coulomb interaction is strong between electron and hole. This is the case in materials with a low dielectric constant and can e.g. be found in organic semiconductor crystals. In inorganic semiconductors we usually have a high dielectric constant and the interaction between the charges is screened, leading to Wannier-Mott excitons. The binding energy of a Wannier-Mott exciton is only a few meV in contrast to a Frenkel exciton which can have binding energies up to several hundred meV.

2.3.2. Effective Mass

With quantum mechanics we can calculate the equation of motion for an electron in a crystal with an applied electric field \mathbf{E} as

$$\frac{d^2\mathbf{r}}{dt^2} = \frac{1}{\hbar^2} \frac{d^2 E(k)}{dk^2} q \mathbf{E}, \quad (2.28)$$

where $E(k)$ is the energy as function of the wavenumber of the electron [17]. If we compare this with the equation of motion for a free electron in an electric field

$$\frac{d^2\mathbf{r}}{dt^2} = \frac{1}{m} q \mathbf{E}, \quad (2.29)$$

we see that we can describe the electron in the crystal as a free electron with a modified mass

$$m^* = \left(\frac{1}{\hbar^2} \frac{d^2 E(k)}{dk^2} \right)^{-1}, \quad (2.30)$$

which is called the *effective mass* of the electron.

Since any smooth function can be approximated by a parabola near a local extremum and the second derivative of a parabola is constant we can assume a constant effective mass for our charge carriers. This assumption is justified because any excess energy that a hole or electron might have directly after the excitation will be transferred to the crystal lattice. This process happens rapidly compared to the lifetime of the exciton, and therefore the exciton will spend most

2. Basic Principles

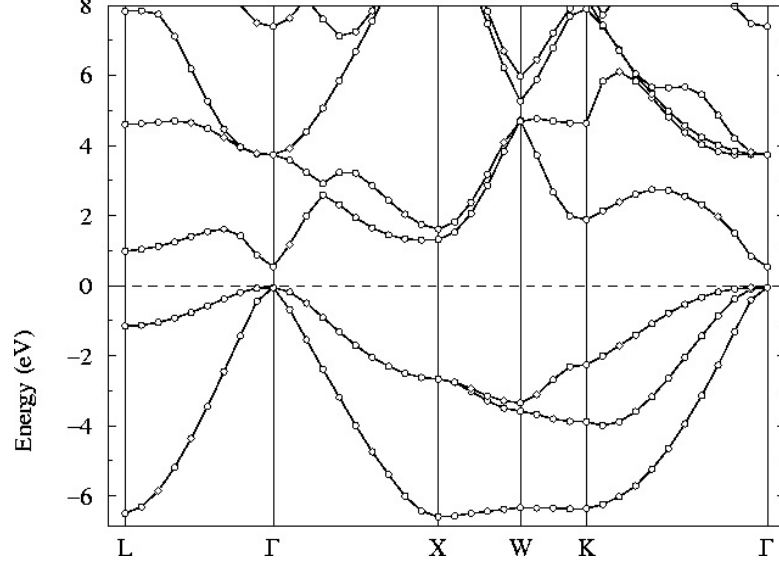


Figure 2.5.: Band structure of Gallium-Arsenide. The physical processes we are considering take place at the maximum of the valence band and the minimum of the conduction band.

of its lifetime in its lowest possible energy state. Because the conduction band is empty or at least sparsely populated the lowest possible energy state is at the band minimum.

2.3.3. Interband Polarization

As discussed in the exciton section an excitation of an electron into the conduction band is accompanied by a separation of charge which leads to a polarization of the material, the so called *interband polarization*. The polarization is the expectation value of the electric dipole operator $e\mathbf{r}$

$$\mathbf{P}(t) = \sum_S \int \langle \Psi_S^\dagger(\mathbf{r}, t) e\mathbf{r} \Psi_S(\mathbf{r}, t) \rangle d\tau, \quad (2.31)$$

where the field operators $\Psi_S^\dagger(\mathbf{r}, t)$ and $\Psi_S(\mathbf{r}, t)$ describe the creation and annihilation of an electron with spin S at position \mathbf{r} . In spatially homogeneous systems the field operators can be expanded in terms of Bloch functions ψ_λ

2. Basic Principles

$$\Psi_S(\mathbf{r}, t) = \sum_{\lambda, \mathbf{k}} a_{\lambda, \mathbf{k}, S}(t) \psi_{\lambda}(\mathbf{k}, \mathbf{r}), \quad (2.32)$$

where λ is the band index. Inserting this into (2.31) we get

$$\mathbf{P}(t) = \sum_{\lambda, \lambda', \mathbf{k}, \mathbf{k}'} \langle a_{\lambda, \mathbf{k}}^{\dagger} a_{\lambda', \mathbf{k}'} \rangle \int \psi_{\lambda, \mathbf{k}}^*(\mathbf{r}) \mathbf{e} \mathbf{r} \psi_{\lambda', \mathbf{k}'}(\mathbf{r}) d\tau, \quad (2.33)$$

where we incorporated the spin index into the summation over \mathbf{k} . The integral over the Bloch functions can be calculated generally[16] and gives

$$\int \psi_{\lambda, \mathbf{k}}^*(\mathbf{r}) \mathbf{e} \mathbf{r} \psi_{\lambda', \mathbf{k}'}(\mathbf{r}) d\tau = \delta_{\mathbf{k}, \mathbf{k}'} \mathbf{d}_{\lambda \lambda'}, \quad (2.34)$$

with the dipole moment $\mathbf{d}_{\lambda, \lambda'}$ that is associated with the respective interband transition. We restrict our treatment to the transition between valence and conduction band and get for the interband polarization

$$\mathbf{P}(t) = \sum_{\mathbf{k}} \langle a_{c, \mathbf{k}}^{\dagger} a_{v, \mathbf{k}} \rangle \mathbf{d}_{cv} + c.c. . \quad (2.35)$$

2.4. Nano and Quantum optics

Applying quantum mechanics to optical phenomena led to many new insights and applications during the last century, the most prominent certainly being the invention of the laser. A fully quantum mechanical approach would require to quantize the particles and the electromagnetic fields. In this thesis we choose a semi classical approach where we treat the exciton as a quantum emitter but do not quantize the radiating field. Textbooks that discuss quantum optics are e.g. [18] and [16].

2.4.1. Dipole Approximation

Typically the size of an atom is small compared to the wavelengths of the light that performs the transitions between different atomic energy levels. Thus the variation of the electric field over the extent of the atom almost does not vary. So we have $\mathbf{k} \cdot \mathbf{r} \ll 1$ and we can expand the electric field in a power series

$$\mathbf{E}(\mathbf{r}, t) = \mathbf{E}(t)e^{-i\mathbf{k} \cdot \mathbf{r}} = \mathbf{E}(t)(1 - i\mathbf{k} \cdot \mathbf{r} + \dots) \quad (2.36)$$

and only take the leading term of the expansion. This is known as the *electric dipole approximation*.

Taking only the leading term is equivalent to neglecting the momentum of the photon, $\mathbf{k} \rightarrow 0$, especially in comparison to the electron momentum. This means that only vertical transitions are allowed in a band diagram like Fig. 2.5.

2.4.2. Rotating Wave Approximation

If we consider an optical two level system with the frequency ω corresponding to the transition between the states driven by an electrical field

$$\mathbf{E}(t) = \mathbf{E}_0 e^{-i\omega t} + \mathbf{E}_0^* e^{i\omega t}, \quad (2.37)$$

the interaction Hamiltonian within the dipole approximation is $H_{op} = -\mathbf{d} \cdot \mathbf{E}$, where \mathbf{d} is the dipole moment of the transition between the states. Therefore we can write the interaction Hamiltonian for a two state system as

$$H_{op} = -(|2\rangle \langle 1| \mathbf{d}_{21} + |1\rangle \langle 2| \mathbf{d}_{21}^*)(\mathbf{E}_0 e^{-i\omega t} + \mathbf{E}_0^* e^{i\omega t}) \quad (2.38)$$

where we used $d_{12} = d_{21}^*$. If we transform this Hamiltonian in the interaction picture with the transformation $U = e^{iH_0 t} = e^{i\omega_0 t|2\rangle \langle 2|}$, we obtain

2. Basic Principles

$$\begin{aligned}
 H_{op,I} = UH_{op}U^\dagger = & -|2\rangle\langle 1|(\mathbf{d}\cdot\mathbf{E}_0 e^{-i(\omega-\omega_0)t} + \mathbf{d}\cdot\mathbf{E}_0^* e^{i(\omega+\omega_0)t}) \\
 & -|1\rangle\langle 2|(\mathbf{d}^*\cdot\mathbf{E}_0 e^{-i(\omega+\omega_0)t} + \mathbf{d}^*\cdot\mathbf{E}_0^* e^{i(\omega-\omega_0)t}).
 \end{aligned}
 \tag{2.39}$$

If the frequency of the electric field is near the resonance, the terms with $(\omega - \omega_0)$ become nearly time independent, whereas the counter rotating terms $(\omega + \omega_0)$ oscillate rapidly and average out to zero on the timescales we are interested in. If we neglect these fast oscillating terms we arrive at the *rotating wave approximation*

$$H_{op,I} = -|2\rangle\langle 1|\Omega e^{-i(\omega-\omega_0)t} - |1\rangle\langle 2|\Omega^* e^{i(\omega-\omega_0)t},
 \tag{2.40}$$

with $\Omega = \mathbf{d}\cdot\mathbf{E}_0$ being the *Rabi frequency*.

2.4.3. Cross sections

This section deals with the absorption and scattering cross sections for nanoparticles. It mainly follows the derivations in [19].

We define the scattering cross section as the power of the scattered electromagnetic field integrated over a sphere around the scattering particle divided by the power of the incoming field. The energy flux of an electromagnetic wave is given by the *Poynting vector*

$$\mathbf{S} = \frac{c}{4\pi} \mathbf{E} \times \mathbf{B},
 \tag{2.41}$$

which points in the propagation direction of the wave. For a plane wave the time average of its magnitude is given by

$$\langle S \rangle = \frac{c}{8\pi} \mathbf{E}^2.
 \tag{2.42}$$

This quantity is also called intensity.

If we apply a field \mathbf{E}_0 to a particle it induces a dipole moment \mathbf{d}

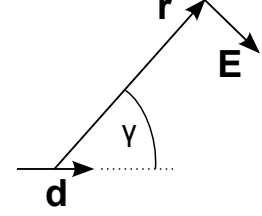
$$\mathbf{d} = \alpha \mathbf{E}_0.
 \tag{2.43}$$

2. Basic Principles

Here α is the *polarizability* a tensor that links the dipole moment to the applied field. The polarizability may be complex and depend on frequency if we consider an electromagnetic wave as the applied field.

A driven oscillating dipole radiates in all directions, which is the so-called *Rayleigh scattering*. The electric field scattered by the dipole at a distance r far away ($r \gg \lambda$) is given by

$$E_{sca} = \frac{k^2 |\mathbf{d}| \sin \gamma}{r} e^{ikr}, \quad (2.44)$$



γ is the angle between the dipole and the direction to the point of measurement [5]. The scattered electric field is oriented perpendicular to \mathbf{r} and lies in the same plane as the dipole.

Figure 2.6.: Electric dipole scattering.

If we integrate the intensity of the scattered wave over a sphere we get the total energy scattered per unit time

$$P_{sca} = \frac{1}{3} k^4 c |\mathbf{d}|^2. \quad (2.45)$$

Dividing this by the intensity of the incoming wave and assuming the amplitude of \mathbf{E}_0 as unity, which we do in all our simulations, we obtain the *scattering cross section*

$$C_{sca} = \frac{8\pi}{3} k^4 |\mathbf{d}|^2. \quad (2.46)$$

We can get the absorbed power if we integrate the total intensity over a surface containing the scattering particle. With total intensity we mean the intensity of the superposition of incoming and scattered field

$$\mathbf{E}_{tot} = \mathbf{E}_0 + \mathbf{E}_{sca}. \quad (2.47)$$

If the above mentioned integration does not evaluate to zero, there has to be an energy sink inside the surface, meaning that the particle has to absorb energy. Although the integral over a sphere is much tougher in this case because the

2. Basic Principles

electric field is not radially symmetric we can derive the absorption cross section similar to the scattering cross section and arrive at

$$C_{abs} = 4\pi k \operatorname{Im}(\mathbf{e} \cdot \mathbf{d}), \quad (2.48)$$

where \mathbf{e} is the unit vector in direction of the incoming field.

We have now summarized the main ingredients for the derivations and simulations that will follow in the next chapters.

3. Theory

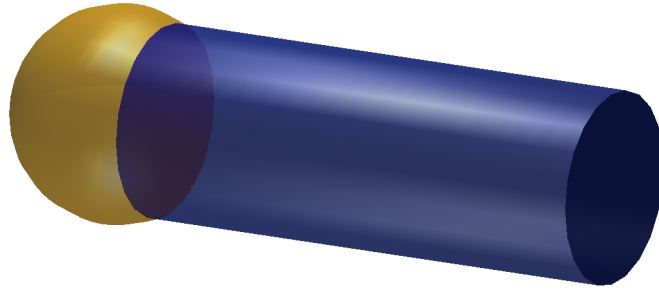


Figure 3.1.: Semiconductor nanorod with attached gold particle.

3.1. Describing the System

The system we investigate in this thesis is a semiconductor-metal nanoparticle embedded in a dielectric environment. The environment is incorporated by classical electromagnetic means and the optical response of the semiconductor is treated in the exciton picture.

The general Hamiltonian of such a system is

$$H = H_0 + H_{eh} + H_{env} + H_{opt} + H_{ee} + H_{hh}, \quad (3.1)$$

where H_0 denote the single particle Hamiltonian for electrons and holes, including kinetic energy and the confinement potential, H_{eh} describes the direct Coulomb

3. Theory

interaction between electron and hole, H_{env} incorporates the Coulomb coupling to the dielectric environment and H_{opt} accounts for optical creation of excitons. H_{ee} and H_{hh} describe the electron-electron and hole-hole interaction, respectively, but we assume a low density of excitons and therefore neglect these interactions in linear response.

In the two band approximation we consider only one electron and one hole band. Thus we can write H_0 in terms of the field operators $\Psi_i^\dagger(\mathbf{r})$ and $\Psi_i(\mathbf{r})$, which create/annihilate an electron or a hole at position \mathbf{r} , as

$$H_0 = \sum_{i=e,h} \int \Psi_i^\dagger(\mathbf{r}) \left(-\frac{\nabla^2}{2m_i} + V_i(\mathbf{r}) \right) \Psi_i(\mathbf{r}) d\tau, \quad (3.2)$$

where m_i denotes the effective mass of an electron or hole in the semiconductor.

The Coulomb term becomes

$$H_{eh} = - \iint G_0(\mathbf{r}, \mathbf{r}') n_e(\mathbf{r}) n_h(\mathbf{r}') d\tau d\tau', \quad (3.3)$$

where the $n_i = \Psi_i^\dagger(\mathbf{r})\Psi_i(\mathbf{r})$ are the electron and hole particle densities and $G_0(\mathbf{r}, \mathbf{r}') = 1/(\epsilon|\mathbf{r}-\mathbf{r}'|)$ is the electrostatic Green's function in an unbound medium. To describe the optical interaction with an external field we use dipole approximation and rotating wave approximation, this leads from (2.40) to

$$H_{op} = - \int \Omega(\mathbf{r}) \Psi_e^\dagger(\mathbf{r}) \Psi_h^\dagger(\mathbf{r}) + \Omega(\mathbf{r})^* \Psi_e(\mathbf{r}) \Psi_h(\mathbf{r}) d\tau. \quad (3.4)$$

Here $\Omega(\mathbf{r}) = \mathbf{d} \cdot \mathbf{E}^+(\mathbf{r})$ is the Rabi energy, with \mathbf{d} the dipole moment associated with the interband transition and \mathbf{E}^+ the external electric field with positive frequency components. The only part that is left now is the interaction with the environment which we describe through the bound charges ρ_b which are induced due to the free charge density ρ_f of electrons and holes. Then this interaction can be written in the form

3. Theory

$$\begin{aligned}
 H_{env} &= \iint G_0(\mathbf{r}, \mathbf{r}') \rho_f(\mathbf{r}) \rho_b(\mathbf{r}') d\tau d\tau' \\
 &= \iint G_0(\mathbf{r}, \mathbf{r}') (\Psi_h^\dagger \Psi_h - \Psi_e^\dagger \Psi_e) \rho_b(\mathbf{r}') d\tau d\tau'.
 \end{aligned}
 \tag{3.5}$$

For the H_{op} and H_{env} we will see a strong influence of the metallic nanoparticle compared to the bare semiconductor. In the environment part the bound charges will be much stronger because the electrons are free within the metal and the optical response will be enhanced due to the field magnification of the particle plasmons.

3.2. Polarization

In a semiconductor electrons and holes are always created pairwise by incident light. Thus, if we assume that in the ground state there are no electrons in the conduction band and the valence band is completely filled, one can show that every n-point function A_n , normal ordered with respect to the exciton-picture, is at least of order m in the electric field [20]. Here $m = \max(n_e, n_h)$ where n_e and n_h are the number of electron and hole field operators in the n-point function. In this thesis we consider the linear response in the electric field therefore the only density matrix we have to treat is the 2-point function *interband polarization* $p(\mathbf{r}, \mathbf{r}') = \langle \Psi_h(\mathbf{r}) \Psi_e(\mathbf{r}') \rangle$. All density matrices of higher order in the electric field will be discarded.

To obtain the equation of motion for the interband polarization we use the Heisenberg equation of motion

$$\frac{d}{dt} p = -\frac{i}{\hbar} [p, H],
 \tag{3.6}$$

the square bracket denoting the commutator of the two operators.

3. Theory

To get the commutators of the field operators with the Hamiltonian we use the anti-commutation relations of fermionic field operators, see for example [21],

$$\{\Psi_i(\mathbf{r}), \Psi_j^\dagger(\mathbf{r}')\} = \delta_{ij}\delta(\mathbf{r} - \mathbf{r}') \quad (3.7)$$

$$\{\Psi_i(\mathbf{r})^\dagger, \Psi_j(\mathbf{r}')^\dagger\} = \{\Psi_i(\mathbf{r}), \Psi_j(\mathbf{r}')\} = 0 \quad (3.8)$$

($i = e, h$), and the fact that we can discard all operators which consist of more than one field operator of the same type after normal ordering. Thereby we get

$$[\Psi_e(\mathbf{r}), H_0] = \left(-\frac{\nabla^2}{2m_e} + V_e(\mathbf{r}) \right) \Psi_e(\mathbf{r}), \quad (3.9)$$

$$[\Psi_e(\mathbf{r}), H_{eh}] = - \int G_0(\mathbf{r}, \mathbf{r}') \rho_h \Psi_e(\mathbf{r}) d\tau', \quad (3.10)$$

$$[\Psi_e(\mathbf{r}), H_{env}] = - \int G_0(\mathbf{r}, \mathbf{r}') \rho_b \Psi_e(\mathbf{r}) d\tau', \quad (3.11)$$

$$[\Psi_e(\mathbf{r}), H_{op}] = -\Omega(\mathbf{r})\Psi_h^\dagger(\mathbf{r}). \quad (3.12)$$

The commutation relations for the hole operators are analog, just the sign in the equations with H_{env} and H_{op} changes. After using the product relation for commutators

$$[AB, C] = A[B, C] + [A, C]B, \quad (3.13)$$

we can arrange the field operators in normal order and then neglect again all the terms that correspond to $\mathcal{O}(E^2)$. Hence we obtain

$$\begin{aligned} i \frac{d}{dt} p &= \left(-\frac{\nabla_e^2}{2m_e} + V_e(\mathbf{r}_e) - \frac{\nabla_h^2}{2m_h} + V_h(\mathbf{r}_h) - G_0(\mathbf{r}_e, \mathbf{r}_h) \right) p(\mathbf{r}_e, \mathbf{r}_h) \\ &- \int (G_0(\mathbf{r}_e, \mathbf{r}) - G_0(\mathbf{r}_h, \mathbf{r})) \langle \Psi_h(\mathbf{r}_h) \rho_b(\mathbf{r}) \Psi_e(\mathbf{r}_e) \rangle d\tau - \langle \Psi_h(\mathbf{r}_h) \Psi_h^\dagger(\mathbf{r}_h) \rangle \Omega(\mathbf{r}_e, t). \end{aligned} \quad (3.14)$$

From (3.7) it follows that the last term is simply $\delta(\mathbf{r}_e - \mathbf{r}_h)\Omega(\mathbf{r}_e, t)$. The second term describes the coupling to the environment. In the integral we can replace

3. Theory

(see section A.2)

$$G_0 \rho_b = \left(\frac{G}{\epsilon} - G_0 \right) \rho_f = \left(\frac{G}{\epsilon} - G_0 \right) (-\Psi_e^\dagger \Psi_e + \Psi_h^\dagger \Psi_h), \quad (3.15)$$

where G is the full electrostatic Green's function incorporating the geometry of the media. After invoking the commutation relations again we can finally write down the equation of motion for the polarization in the linear field limit

$$i \frac{d}{dt} p(\mathbf{r}_e, \mathbf{r}_h) = \left(-\frac{\nabla_e^2}{2m_e} + V_e(\mathbf{r}_e) - \frac{\nabla_h^2}{2m_h} + V_h(\mathbf{r}_h) - \frac{G(\mathbf{r}_e, \mathbf{r}_h)}{\epsilon} \right) p(\mathbf{r}_e, \mathbf{r}_h) - \delta(\mathbf{r}_e - \mathbf{r}_h) \Omega(\mathbf{r}_e, t). \quad (3.16)$$

3.3. Optical response

To calculate the scattering and absorption spectra of the hybrid particle we have to identify the contributions of all the different processes to the dipole moment \mathbf{d} and electric field \mathbf{E} in equations (2.46) and (2.48).

For our further derivations we use exciton wave functions ψ which have to obey the Schrödinger equation

$$\left(-\frac{\nabla_e^2}{2m_e} + V_e(\mathbf{r}_e) - \frac{\nabla_h^2}{2m_h} + V_h(\mathbf{r}_h) - \frac{G(\mathbf{r}_e, \mathbf{r}_h)}{\epsilon} \right) \psi = \varepsilon \psi. \quad (3.17)$$

It is shown in section A.3 how they can be calculated. Since the exciton wave functions form an orthonormal set we can expand $p(\mathbf{r}, \mathbf{r}')$ as

$$p(\mathbf{r}, \mathbf{r}') = \sum_{\lambda} c_{\lambda} \psi_{\lambda}(\mathbf{r}, \mathbf{r}'). \quad (3.18)$$

Inserting this into (3.16) and assuming a harmonic driving field with frequency ω we get

$$\omega \sum_{\lambda} c_{\lambda} \psi_{\lambda}(\mathbf{r}_e, \mathbf{r}_h) = -\delta(\mathbf{r}_e - \mathbf{r}_h) \Omega(\mathbf{r}_e) + \sum_{\lambda} c_{\lambda} \varepsilon_{\lambda} \psi_{\lambda}(\mathbf{r}_e, \mathbf{r}_h) \quad (3.19)$$

3. Theory

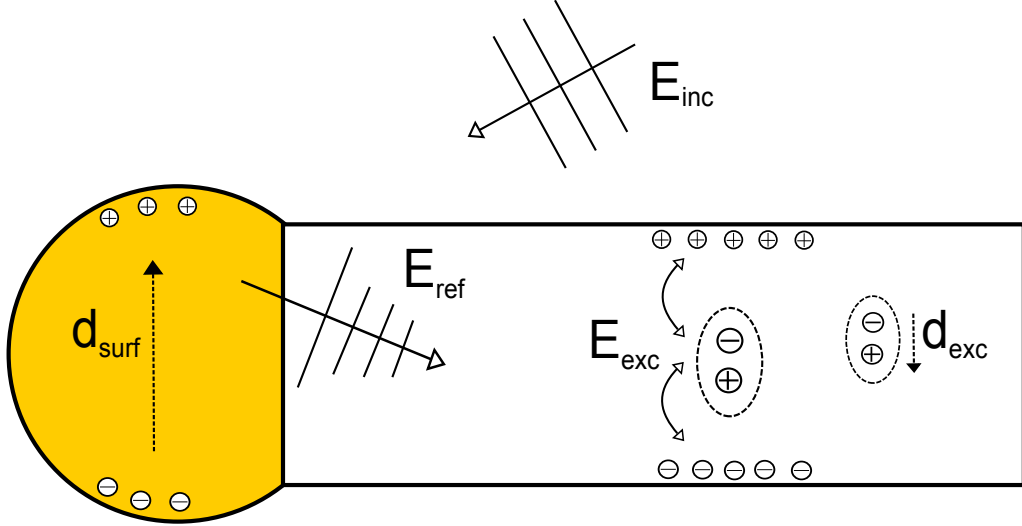


Figure 3.2.: Fields and dipole moments. We have an incoming plane wave excitation \mathbf{E}_{inc} , a field generated by polarization of the material \mathbf{E}_{ref} which is dominated by the evanescent plasmon field and a dipole field of the exciton \mathbf{E}_{exc} which also polarizes the surrounding media. The induced surface charges exhibit a dipole moment \mathbf{d}_{surf} as well as the exciton itself \mathbf{d}_{exc} .

because the exciton wave functions are the eigenfunctions of the Hamiltonian in (3.16). To determine the coefficients we modify the previous equation by calculating the scalar product with $\psi_{\mu}^*(\mathbf{r}_e, \mathbf{r}_h)$ and using orthonormality of the wave functions

$$(\omega - \varepsilon_{\mu})c_{\mu} = - \int \Omega(\mathbf{r})\psi_{\mu}(\mathbf{r}_e, \mathbf{r}_h). \quad (3.20)$$

To solve this equation we have to take a closer look at the electric field that occurs in the Rabi energy. It is composed of the external field, the field reflected by the surface, which is dominated by the evanescent field of the plasmon, and the dipole self interaction of the exciton as shown in Fig. 3.2,

$$\Omega(\mathbf{r}) = \mathbf{d} \cdot [\mathbf{E}_{inc} + \mathbf{E}_{ref}(\mathbf{r}) + \mathbf{E}_{exc}(\mathbf{r})]. \quad (3.21)$$

Since $\mathbf{d}p(\mathbf{r}, \mathbf{r})$ is the interband dipole at \mathbf{r} the self induced field of the exciton can be expressed as

3. Theory

$$\mathbf{E}_{exc}(\mathbf{r}) = k^2 \int \overleftrightarrow{\mathbf{G}}(\mathbf{r}, \mathbf{r}') \mathbf{d} \sum_{\mu} c_{\mu} \psi_{\mu}(\mathbf{r}', \mathbf{r}') d\tau, \quad (3.22)$$

where $\overleftrightarrow{\mathbf{G}}(\mathbf{r}, \mathbf{r}')$ is the dyadic Green's function that relates a dipole at \mathbf{r}' to its reflected field at \mathbf{r} via the environment, which lets us define the term

$$K_{\mu\mu'} = k^2 \int \psi_{\mu}(\mathbf{r}, \mathbf{r}) \mathbf{d}(\mathbf{r}) \cdot \overleftrightarrow{\mathbf{G}}(\mathbf{r}, \mathbf{r}') \cdot \mathbf{d}(\mathbf{r}') \psi_{\mu'}(\mathbf{r}', \mathbf{r}') d\tau d\tau'. \quad (3.23)$$

Together with the additional substitution

$$\Omega_{\mu} = \int \mathbf{d} \cdot [\mathbf{E}_{inc} + \mathbf{E}_{ref}(\mathbf{r})] \psi_{\mu}(\mathbf{r}, \mathbf{r}) d\tau \quad (3.24)$$

we can rewrite (3.20) as

$$(\omega - \varepsilon_{\mu}) c_{\mu} = -\Omega_{\mu} - \sum_{\mu'} K_{\mu\mu'} c'_{\mu'}, \quad (3.25)$$

which gives a set of linear equations that are easy to solve numerically.

We do not only have to split up the electric field but also have to consider what the involved dipoles, that interact with those fields, are. First of all we consider the dipole moment exhibited by the surface charge of the particle

$$\mathbf{d}_{surf} = \int_{\partial V} \sigma(\mathbf{s}) \mathbf{s} da = \int_{\partial V} [\sigma_{inc}(\mathbf{s}) + \sigma_{exc}(\mathbf{s})] \mathbf{s} da, \quad (3.26)$$

where σ_{inc} is the surface charge induced by the incoming electric field, selfconsistently incorporating the reflected field of the metallic nanoparticle, and σ_{exc} is the surface charge generated by the exciton. The other dipole moment we consider is that of the exciton, i.e. the integral over the polarization

$$\mathbf{d}_{exc} = \sum_{\mu} \int \mathbf{d} c_{\mu} \psi_{\mu}(\mathbf{r}, \mathbf{r}) d\tau. \quad (3.27)$$

We now have all the ingredients needed to calculate the spectra of the particle:

3. Theory

$$C_{sca} = \frac{8\pi}{3} k^4 |\mathbf{d}_{surf} + \mathbf{d}_{exc}|^2 \quad (3.28)$$

and

$$C_{abs} \propto \text{Im}\{\mathbf{E}_{inc} \cdot \mathbf{d}_{surf} + \sum_{\mu} c_{\mu} \int \psi_{\mu}(\mathbf{r}, \mathbf{r}) \mathbf{d} \cdot [\mathbf{E}_{inc} + \mathbf{E}_{ref}(\mathbf{r}) + \mathbf{E}_{exc}(\mathbf{r})] d\tau\}. \quad (3.29)$$

If we take a closer look at the integral in the absorption cross section we see that it is the same as the right hand side of (3.20) except for the sign. We can therefore write a simpler expression

$$C_{abs} = 4\pi k \text{Im}\{\mathbf{E}_{inc} \cdot \mathbf{d}_{surf} - \sum_{\mu} c_{\mu}^2 (\omega - \varepsilon_{\mu})\}. \quad (3.30)$$

With these results we conclude this chapter and go on to show the numerical means we used to calculate the quantities which occurred in our derivations so far.

4. Numerics

Solving Maxwell's equations and calculating the Green's functions is not possible for arbitrary particle geometries and we have to resort to numerics to treat our system. This chapter will give an overview of the used numerical techniques. All computations and the visualizations were done in Matlab with excessive use of the MNPBEM toolbox [1]. This is a toolbox to simulate metallic nanoparticles with the boundary element method which we will explain shortly. Other methods of solving Maxwell's equations may be found in [22], for example.

4.1. Discretizing the Hamiltonian

Since the interaction of the charges with the dielectric media is not solvable analytically we had to use a grid for our Hamiltonian. We chose a 3-dimensional Cartesian grid and incorporated the Laplace operator via finite differences method

$$\nabla^2 f(\mathbf{r}) = \sum_i \frac{f(r_1, \dots, r_i + h, \dots) + f(r_1, \dots, r_i - h, \dots) - 2f(r_1, \dots, r_i, \dots)}{h_i^2} \quad (4.1)$$

and periodic boundary conditions for the grid. For the confinement we set the points inside the semiconductor to the negative value of the confinement potential and the points outside to zero.

4.2. Boundary Element Method

The Boundary Element Method (BEM) is a method to solve Maxwell's equations developed by Garcia de Abajo and Howie [2]. As the name suggests, this tech-

4. Numerics

nique just discretizes the boundaries of a body rather than the whole volume of the particle, as done in Discrete Dipole Approximation (DDA), lowering the requirements for CPU time and memory. The catch is that it does not apply to arbitrary dielectric environments but one has to make the following assumptions for the involved media:

- homogeneous isotropic dielectric functions
- sharp boundaries between different media

But these assumptions are satisfied for most systems involving plasmonics, especially the systems covered in this thesis.

4.2.1. BEM theory

As we already mentioned, a solution to the Poisson equation (2.9) in the quasistatic approximation can be written as

$$\phi(\mathbf{r}) = \phi_{ext}(\mathbf{r}) + \oint_{V_i} G(\mathbf{r}, \mathbf{s}) \sigma(\mathbf{s}) da. \quad (4.2)$$

ϕ_{ext} is the external potential and $\sigma(\mathbf{s})$ the charge density at the boundary of medium i . This solution fulfills (2.9) everywhere except at the boundaries of different media. Therefore we have to choose the surface charge σ so that the boundary conditions of Maxwell's equations (see Appendix A.1) are fulfilled. From condition (A.11) follows that the charge density has to be the same on both sides of the surface. For the second condition (A.12) we require the surface derivative of the potential

$$\lim_{\mathbf{r} \rightarrow \mathbf{s}} \mathbf{n} \cdot \nabla \phi(\mathbf{r}) = \lim_{\mathbf{r} \rightarrow \mathbf{s}} \frac{\partial \phi(\mathbf{r})}{\partial n} = \lim_{\mathbf{r} \rightarrow \mathbf{s}} \left\{ \frac{\partial}{\partial n} \int_{\partial V} G(\mathbf{r}, \mathbf{s}') \sigma(\mathbf{s}') da' + \frac{\partial \phi_{ext}(\mathbf{r})}{\partial n} \right\}. \quad (4.3)$$

But we have to take care of the singularity in the Green's function at $\mathbf{s}' \rightarrow \mathbf{s}$. If one assumes a homogeneous charge density on a small area around \mathbf{s} the integral

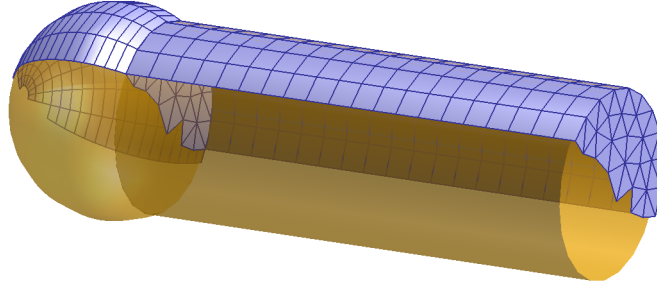


Figure 4.1.: Surface discretization. Every interface between different media is split into small planar polygons.

evaluates to $\pm 2\pi\sigma(\mathbf{s})$, the sign depending on the direction from which the surface is approached[13]. The whole expression then reads

$$\lim_{\mathbf{r} \rightarrow \mathbf{s}} \mathbf{n} \cdot \nabla \phi(\mathbf{r}) = \frac{\partial \phi(\mathbf{s})}{\partial n} = \int_{\partial V} F(\mathbf{s}, \mathbf{s}') \sigma(\mathbf{s}') da' \pm 2\pi\sigma(\mathbf{s}) + \frac{\partial \phi_{ext}(\mathbf{s})}{\partial n} \quad (4.4)$$

where $F = \partial_n G$ and the surface integral excludes a small area around \mathbf{s} . Now we are almost finished because this equation can be solved after discretizing the boundary.

4.2.2. Surface discretization

Since equation (4.4) is only solvable analytically for very few geometries, e.g. spheres [23], we have to discretize the surface and split it into small planar faces. We take all surface elements small enough to justify the assumption of homogeneous charge density throughout each face and can then rewrite equation (4.4) in discretized form

$$\left(\frac{\partial \phi(\mathbf{s})}{\partial n} \right)_i = \sum_j F_{ij} \sigma_j \pm 2\pi\sigma_i + \frac{\partial \phi_{ext}}{\partial n}. \quad (4.5)$$

Inserting this vector equation into the boundary condition (A.12) we can simply calculate the surface charge by matrix inversion

4. Numerics

$$\boldsymbol{\sigma} = -(\hat{\mathbf{\Lambda}} - \hat{\mathbf{F}})^{-1} \frac{\partial \phi_{ext}}{\partial n}, \quad (4.6)$$

with

$$\hat{\mathbf{\Lambda}} = 2\pi \frac{\epsilon_2 + \epsilon_1}{\epsilon_2 - \epsilon_1} \mathbb{1}$$

a matrix that incorporates the dielectric functions of the adjacent media.

With the knowledge of the surface charge we can compute the potentials, e.g. by (2.2), and fields everywhere else. If we want to know the fields or potentials far away, we simply put the charges in the middle of each face and treat them like point charges. If we look closely to a particle surface we have to smear out the charge over the face and integrate over the charge distribution to get accurate results.

4.3. Program outline

This section outlines the structure of our approach. The approach can be divided into three main parts:

- Initialization of particle:
Setting the geometry and discretization of the particle with MNPBEM toolbox and defining material parameters
- Exciton wave functions:
We start with single particle wave functions of electron and hole calculated by a simple particle-in-a-box approach. Then we calculate their self interaction and mutual interaction, which consists of a direct part and indirect interaction through the environment. From this we then calculate the exciton wave functions. More details can be found in section A.3.
- Optical response:
With the knowledge of the exciton wave functions we can calculate the coefficients for the polarization and therefore calculate the optical response as

4. Numerics

shown in section 3.3. Since the dielectric functions depend on light frequency this calculations have to be looped over all incoming wavelengths.

Before we close this chapter we also want to mention the limiting factors of our numerical approach. For the exciton self interaction we have to consider every point of our space grid as an emitting and absorbing dipole and therefore we have to calculate all the dyadic Green's function for every combination of space points. We also have to consider that many points are very close to the surface and we can not use the approximation of point charges on the surfaces but have to integrate over the homogeneous charge distribution on each surface element in many cases. This two factors lead to a rapid increase of memory and time demands dependent on the grid size. The computations for the optical response part, which is the most time demanding task in this scheme, have to be done separately for each excitation wavelength and the computation time increases linearly with the energy resolution.

5. Results

The semiconductor in our simulations can be modeled by various parameters which are listed in table 5.1. The values we took for the presented results account for Cadmium-Selenide (CdS). For the metallic sphere we used gold. For the respective frequency dependent dielectric functions we used literature values that can be found in [24] for CdS and in [12] for gold. The values we used for the particle geometry are listed in table 5.1 and are explained in Fig. 5.1. The edges of the semiconductor cylinder are rounded to avoid possible singularities. The evanescent field at such an edge would become unrealistically high and the results would be dominated by a few grid points near the edges. We defined the roundness with a parameter d which specifies the difference between the radius of the semiconductor in the middle of the rod and the radius where it touches the gold sphere. We took exactly these particle dimensions to compare our results with [24] and because the exciton energies match the plasmon resonance for these dimensions.

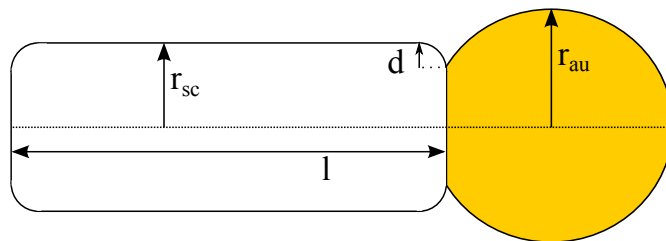


Figure 5.1.: Particle dimensions.

5. Results

Particle parameters	value
dielectric constant of background (toluene)	2.49
radius semiconductor r_{sc}	2.9 nm
length semiconductor l	14 nm
radius gold r_{au}	3 nm
rounding parameter d	0.5 nm
Semiconductor parameters	value
dipole strength	0.5 Debye
band gap	2.420 eV
effective mass electron	0.067 m_e
effective mass hole	0.38 m_e
confinement potential hole	215 meV
confinement potential electron	400 meV

Table 5.1.: Parameters used in our simulations.

5.1. Combining Particles

We will delay the discussion of the exciton behaviour for a while and first of all discuss the optical properties of the particle where the semiconductor is just described with its dielectric function without the exciton. In Fig. 5.2 we compare the scattering and absorption spectra for the individual components with the spectra of the combined particles. As excitation a plane wave polarized along the symmetry axis of the particle was assumed.

First of all we see that the optical response is dominated by the absorption which is about three orders of magnitude stronger than the scattering. We also see that the complete particle response is more than the sum of its parts. The cross sections for the combined particle are larger than the sum of component cross sections. Additionally the resonance frequency of the metallic particle is shifted to lower frequencies in the presence of the semiconductor. These findings match the results of [24] quite well.

5. Results

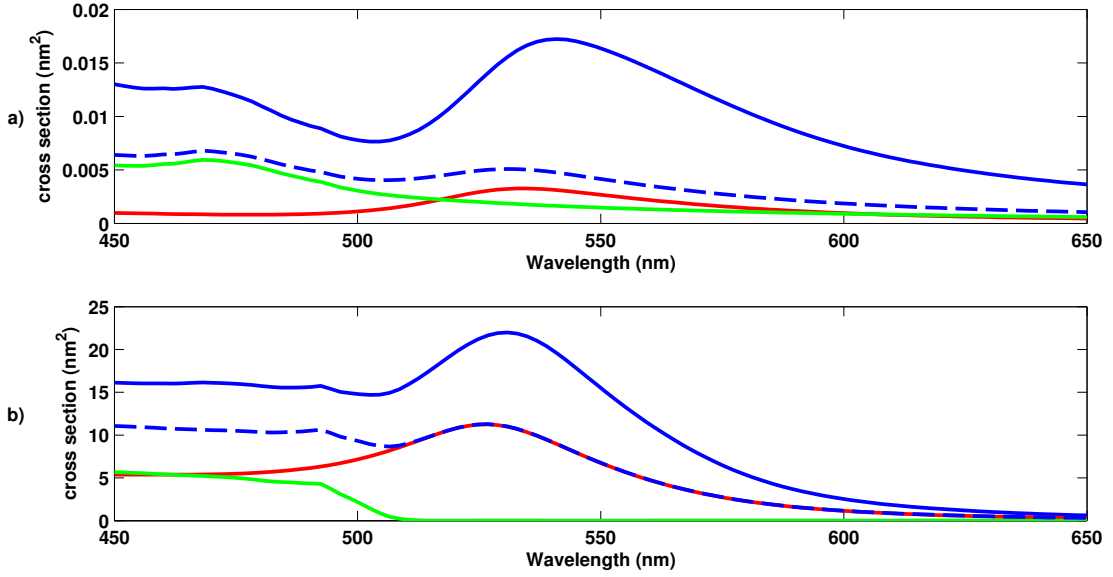


Figure 5.2.: Influence of semiconductor on plasmon behaviour. This graphs compare a) scattering cross section and b) absorption cross section of the constituents and the whole particle. The red line is the bare gold nanoparticle, the green line shows the bare semiconductor rod, the blue line shows the simulation results for the combined hybrid particle and the dashed blue line is the sum of red and green line for comparison.

5.2. Charge carrier densities

The calculations in the previous section can easily be done with the MNPBEM toolbox and it is just a matter of defining the right geometries. The trickier part is to incorporate the excitonic behaviour. For this we had to calculate the densities of the charge carriers. Therefore we take a look at the influence of the surrounding media on the wave functions of the charge carriers. If we look at the figures 5.3 and 5.4, we see that the symmetric wave function of the particle-in-a-box approach for the bare semiconductor is deformed by the interaction with the gold particle. The image charge in the metal attracts the charges and the density shifts towards the tip of the matchstick. Through the inclusion of the electron-hole interaction the charges get attracted to each other and feel the repulsion from the image charge of the opposite charge carrier. We can also see that the hole is stronger localized due to its higher effective mass.

5. Results

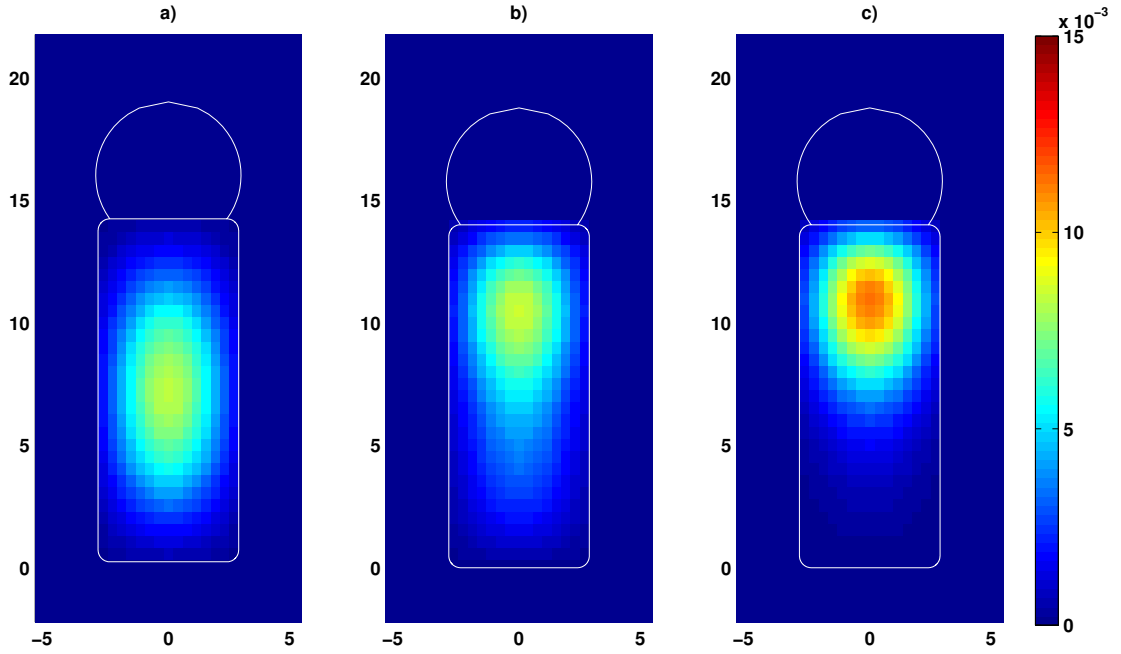


Figure 5.3.: Electron densities. a) charge density in square well potential of electron ground state b) density including self interaction with the environment, c) electron charge density in the exciton ground state.

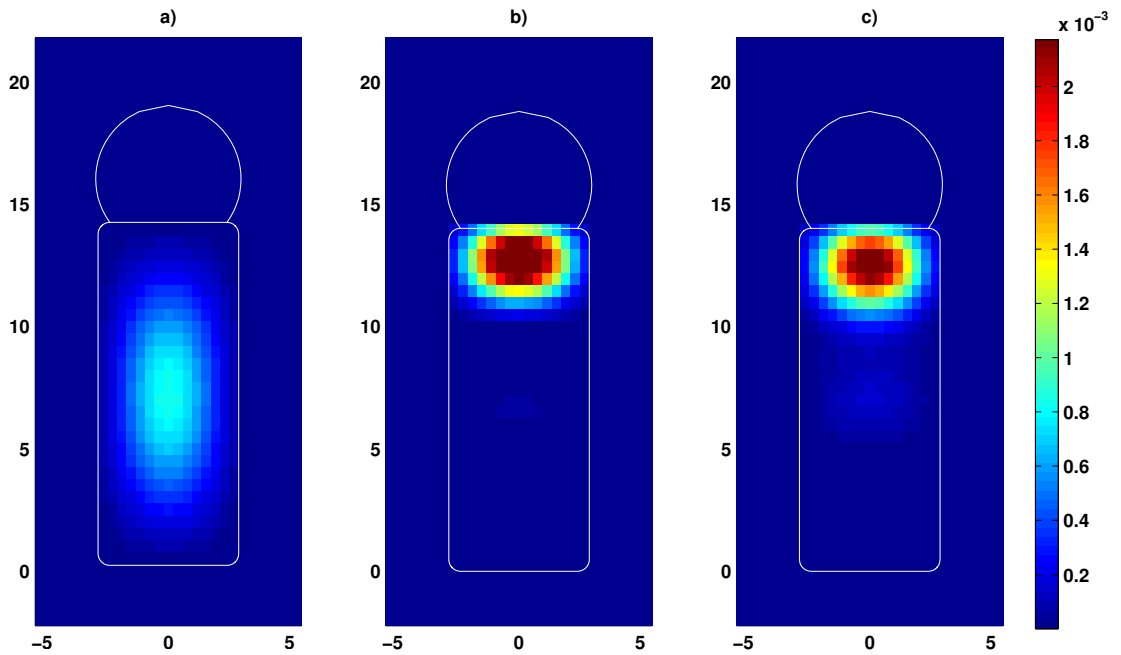


Figure 5.4.: Hole densities. a) charge density in square well potential of electron ground state b) density including self interaction with the environment, c) hole charge density in the exciton ground state.

Together with the exciton wave functions we also calculated the energies for the exciton excitations. Including the semiconductor band gap they lie in the range from 610 nm to 530 nm, approximately matching the plasmon resonance.

5.3. Polarization

An important step to get to the optical properties of the particle is to compute the interband polarization $p(\mathbf{r}, \mathbf{r}) = \sum_{\mu} c_{\mu} \psi_{\mu}(\mathbf{r}, \mathbf{r})$ which is shown in Fig. 5.5 and Fig. 5.6. We calculated the response of the particle for incident light polarized in the same direction as the symmetry axis of the matchstick shaped particle.

Figure 5.5 shows the interband polarization at a wavelength not resonant with the exciton energies and the plasmon peak. In this case we see that the polarization is symmetrically distributed in the semiconductor and the imaginary part, which is connected to the absorption of the particle, is much lower than in Fig. 5.6 which shows the polarization at $\lambda = 650$ nm, the wavelength that matches the lowest exciton state. The second figure also shows that for this wavelength the influence of the plasmon is more pronounced and the semiconductor is stronger polarized in the vicinity of the gold tip.

If we look at the real part of the polarization due to the exciton in Fig. 5.7 we clearly see resonant behaviour at each exciton energy level. For energies higher than a resonance the polarization is phase shifted by 180° and points in the opposite direction of the exciting field. For lower energies polarization and exciting field are in sync. The imaginary part, which is connected to the absorption, only has spikes at the resonances.

5. Results

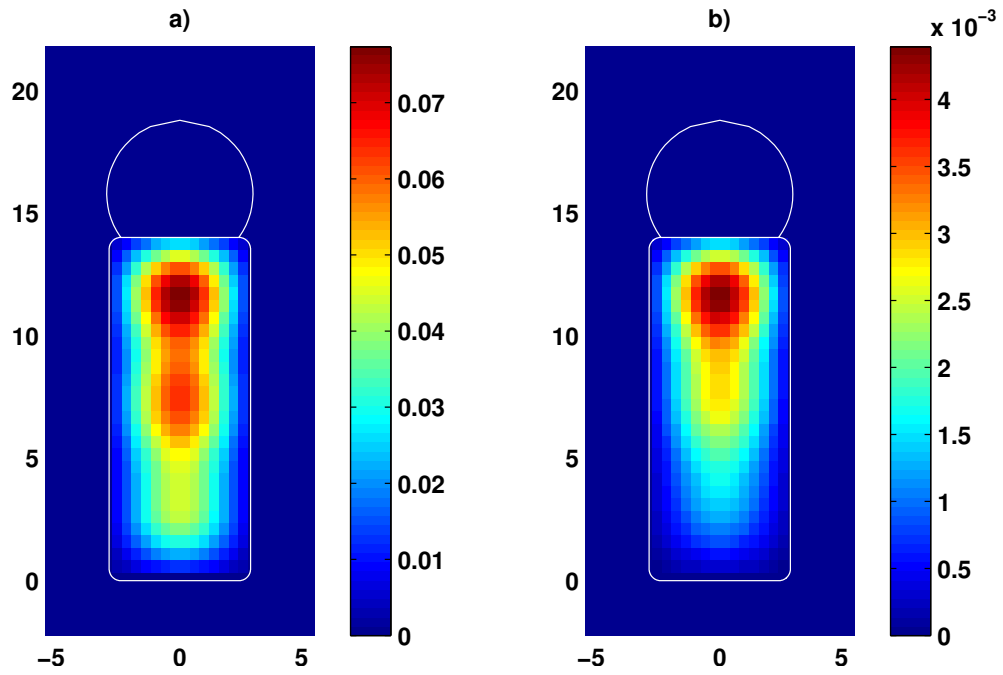


Figure 5.5.: a) real part of polarization and b) imaginary part of polarization for excitation with $\lambda = 650$ nm.

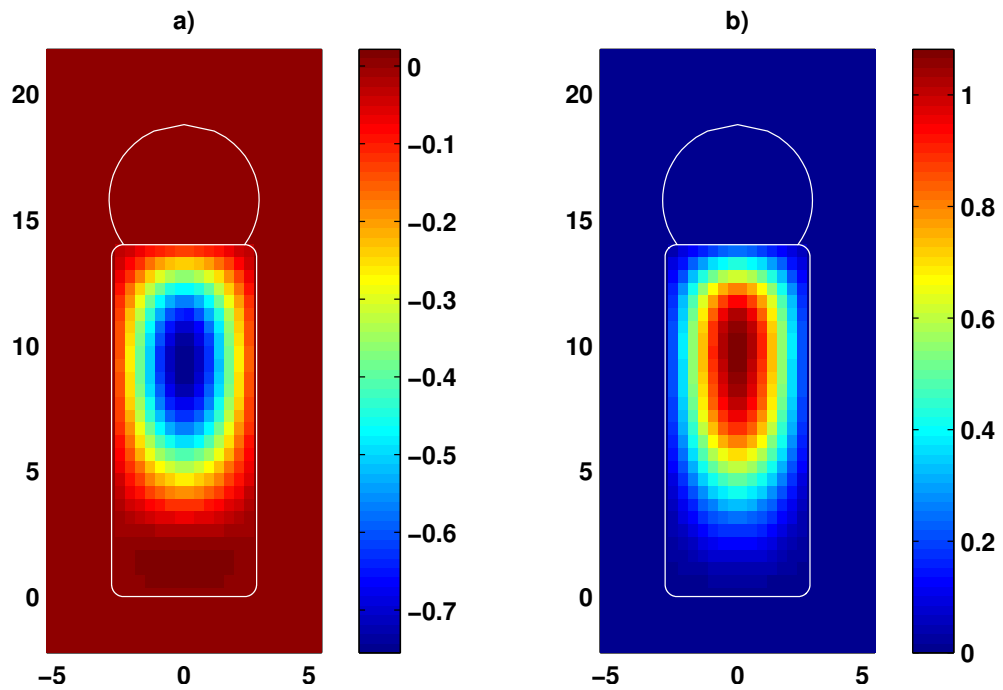


Figure 5.6.: a) real part of polarization and b) imaginary part of polarization for excitation with $\lambda = 608$ nm which is the resonance of the lowest exciton state.

5. Results

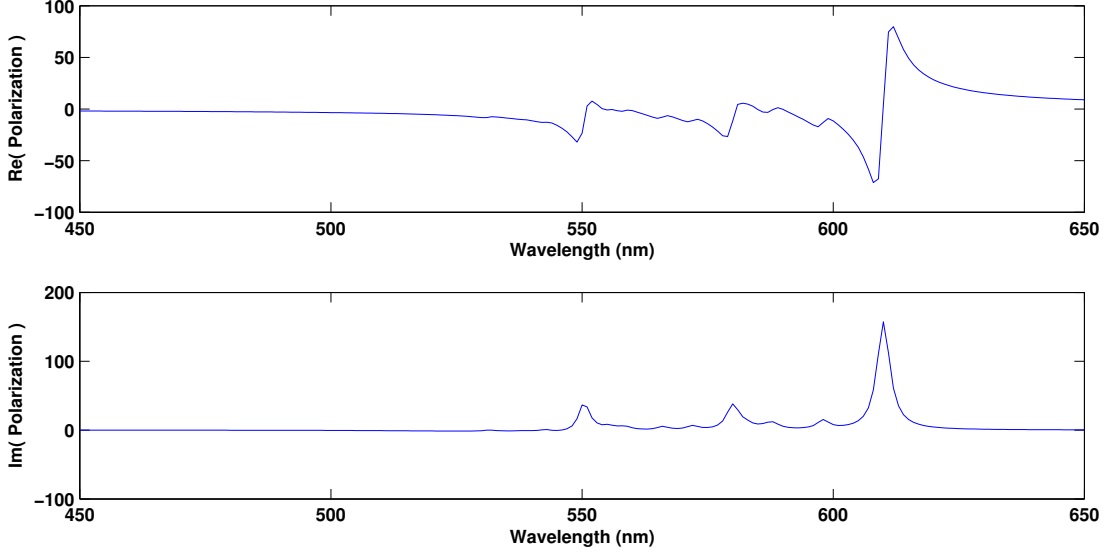


Figure 5.7.: Real and imaginary part of the exciton polarization summed over the whole particle.

5.4. Optical response

This section contains the main goal of the thesis, the optical properties of the hybrid particle including exciton interactions.

In figures 5.8 and 5.9 we compare the optical response of the bare semiconductor rod and the Janus particle this time including excitons. We see that the resonances in the bare semiconductor are at a shorter wavelength, this means that the image charge in the metallic sphere lowers the exciton energies. Further we see that the peaks in absorption and scattering in 5.9 are higher than in 5.8, even if we would subtract the plasmon peak from Fig. 5.2. This is caused by a stronger coupling of the dipole to the exciting field via the evanescent plasmon field.

We also want to identify the effect of the self interaction of the exciton dipole via the environment on the optical response. This is the term that is described by $K_{\mu\mu'}$ in (3.25). Therefore we compare Fig. 5.9 with 5.10 where the optical response with $K_{\mu\mu'} = 0$ is plotted. We see that the self interaction just leads to a damping of the resonances but does not influence their location.

5. Results

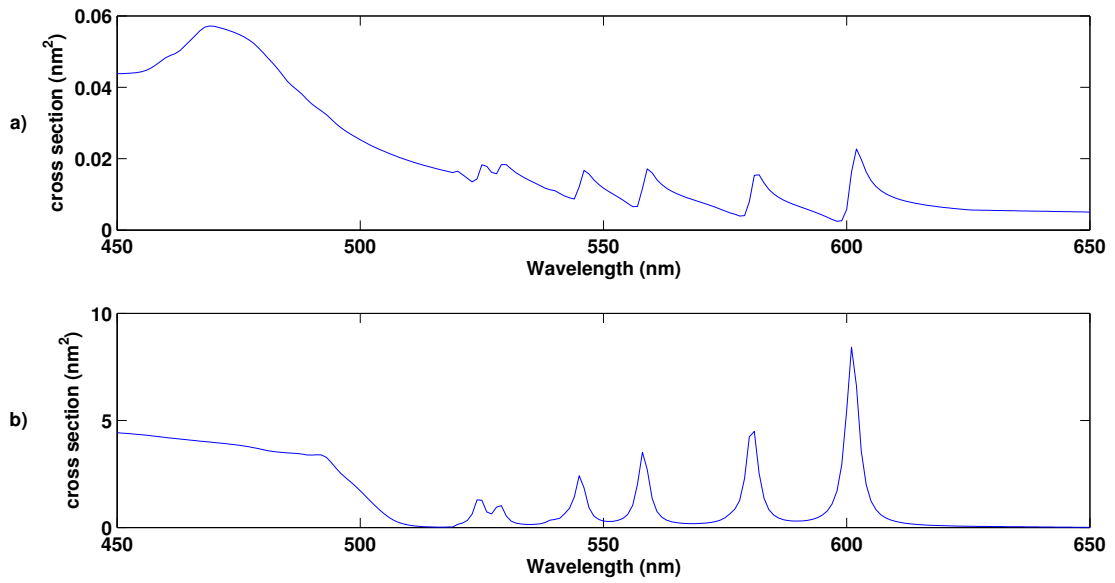


Figure 5.8.: Scattering and absorption spectrum of bare semiconductor rod involving excitons.

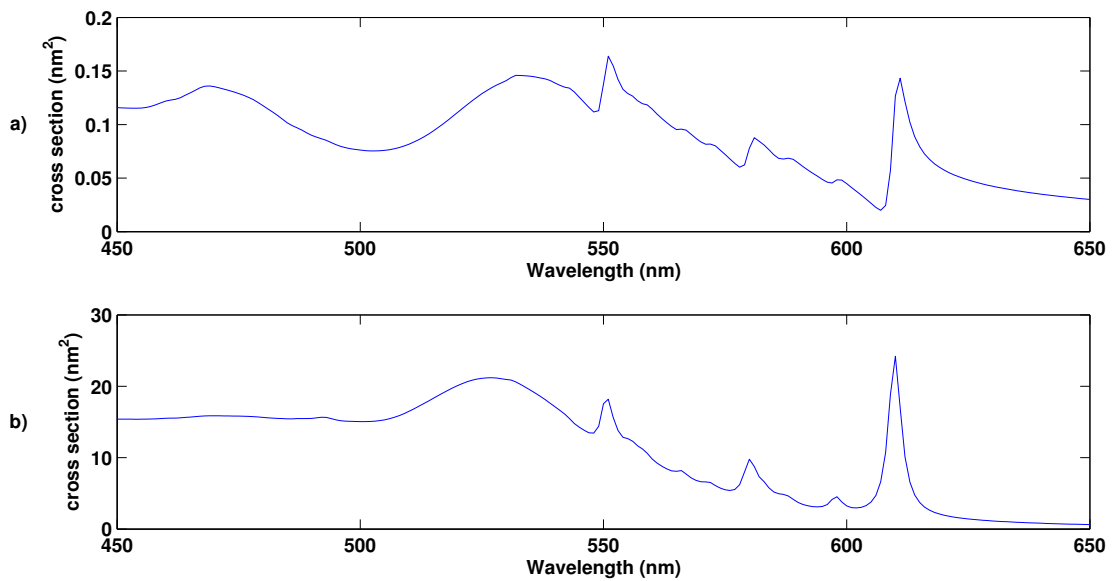


Figure 5.9.: Scattering and absorption of the whole Janus particle including excitons.

5. Results

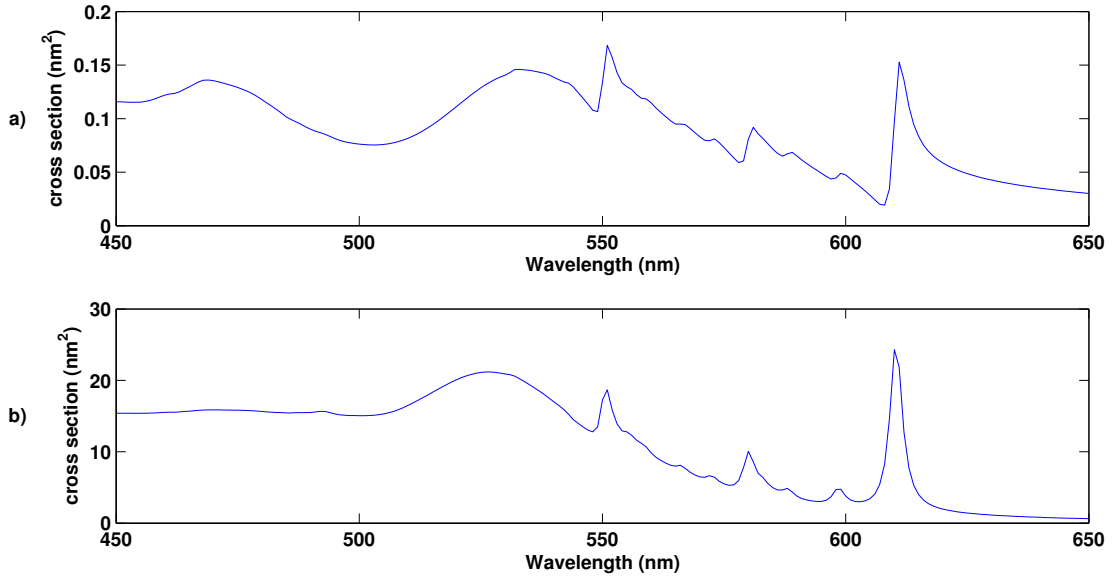


Figure 5.10.: Spectrum without dipole self interaction.

5.5. Influence of numerical parameters

Besides the physical parameters, like size, dielectric function or dipole moment, also numerical parameters may have a big influence on the calculations. To ensure meaningful results we have to check that our numerical approximations have as little influence as possible.

5.5.1. Grid size

The Cartesian grid incorporates the whole particle and about half of the particle size of background in each direction. Therefore the most interesting points that lie inside the particle are about one eighth of number of total points.

To determine a meaningful grid size we used the energy of the lowest state as measure of convergence. For the simulations that led to the presented results, a 30x30x50 grid was used. For these grid parameters the energy levels of the exciton converge. For smaller grids the energies do not converge.

We also determined the energies for much higher grid resolutions, up to 90x90x130, and they are approximately the same as for the used grid parameters. We could

not use this high resolution for the whole calculations because of memory and time limitations.

5.5.2. Number of states

To calculate the exciton wave functions we used products of one particle wave functions of electrons and holes, see equation (A.28). Therefore we needed a numerical cut off for the number of these single particle wave functions. We took all states below the confinement energy because we are only interested in the charges that are confined to the semiconductor (bound states).

5.6. Problems

In the first calculations we used a particle without rounded edges. But sharp edges led to unrealistically high fields. Together with the approximation that was incorporated by the grid approach, grid points near these edges had an disproportionately high influence on the results.

5.7. Conclusion

In this thesis we studied optical properties of a semiconductor-metal hybrid nanoparticle. We developed a scheme to describe the polarization due to the excitons created in the semiconductor within the linear field regime. We used the MNPBEM toolbox [1], that is based on the boundary element method, to derive the Green's functions for our system. With these Green's functions we were able to calculate the exciton wave functions and the polarization dynamics.

In a simple dielectric simulation, neglecting exciton effects, we saw that the scattering and absorption cross section of the combined particle is larger than the sum of the optical response of the different components.

5. Results

We saw that the exciton energies in the combined particle are lowered due to image charges in the metallic particle. This also leads to a stronger localization of the exciton near the metal-semiconductor interface.

As expected the optical response of the excitons mainly depends on the strength of the interband dipole moment \mathbf{d} . Typically it is in the range from 0.1 to 1 Debye. In our calculations we assumed it to be 0.5 Debye. The strength of the exciton resonances also depend on their relative location to the plasmon peak because they are enhanced by the evanescent field of the plasmonic particle. The electron self interaction with the environment, which is described by $K_{\mu\mu'}$, just has a little damping effect but no effect on the resonance frequencies.

Acknowledgements

First of all I want to thank my mother and my grandparents for their great support. You are the ones who made it possible for me to study in this interesting field.

I want to thank Univ. Prof. Ulrich Hohenester for the exceptional supervision. He always had an open door for my questions, was inspiring with his intuition for physics and made it fun to work in his group.

To my colleagues Andi, Toni, Rene and Benedikt i am grateful for their advice and never letting it get too boring in the office. I also want to thank all the friends and fellow students that helped me during the last years and made studying physics interesting and fun. In that regard I especially want to thank Michi and Sebastian with whom i had many entertaining and memorable experiences during this time.

Finally I want to thank Johanna for her love and for kicking me in the butt when I got too lazy.

A. Calculations

A.1. Boundary Conditions

To study the behaviour of the normal component of the electromagnetic field at interfaces between dielectric media we look at equations (2.3a) and (2.3b) in their integral form [4]

$$\oint_S \mathbf{D} \cdot \mathbf{n} \, da = 4\pi \int \rho \, d\tau, \quad (\text{A.1})$$

$$\oint_S \mathbf{B} \cdot \mathbf{n} \, da = 0. \quad (\text{A.2})$$

We now take these integrals over the cylindric volume shown in Fig. A.1 but place some restrictions on that volume. First of all we take the limit $h \rightarrow 0$ for the height of the cylinder and second we take a very thin cylinder, so we can assume constant fields at the top and bottom area of the cylinder and a constant charge density at the interface. In these limits we get for the left hand side of the

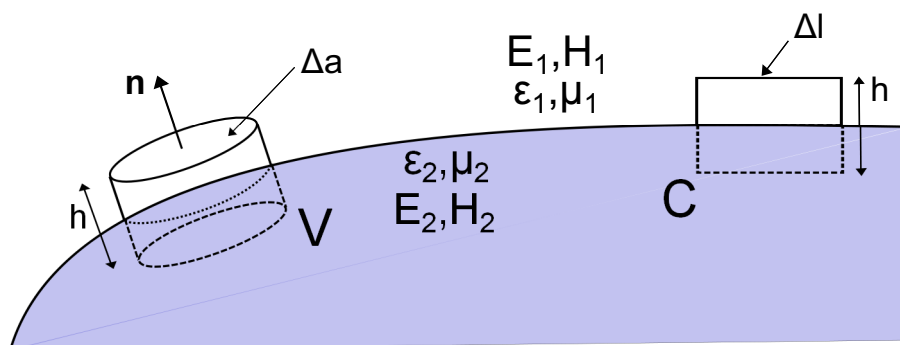


Figure A.1.: Schematics for derivation of boundary conditions for Maxwell's equations

A. Calculations

equations above

$$\oint_S \mathbf{D} \cdot \mathbf{n} da = (\mathbf{D}_1 - \mathbf{D}_2) \cdot \mathbf{n} \Delta a, \quad (\text{A.3})$$

$$\oint_S \mathbf{B} \cdot \mathbf{n} da = (\mathbf{B}_1 - \mathbf{B}_2) \cdot \mathbf{n} \Delta a, \quad (\text{A.4})$$

with the fields in the respective medium, \mathbf{n} the surface normal and Δa the area of the top of the cylinder. On the right hand side of (A.1) we just have to consider the (constant) surface charge density in the limit $h \rightarrow 0$

$$4\pi \int \rho d\tau = 4\pi\sigma\Delta a. \quad (\text{A.5})$$

Therefore we get the boundary conditions for the normal components of the electromagnetic field

$$(\mathbf{D}_1 - \mathbf{D}_2) \cdot \mathbf{n} = 4\pi\sigma, \quad (\text{A.6})$$

$$(\mathbf{B}_1 - \mathbf{B}_2) \cdot \mathbf{n} = 0. \quad (\text{A.7})$$

To get the conditions for the tangential components we take the integral form of (2.3c) and (2.3d)

$$\oint_C \mathbf{H} \cdot d\mathbf{l} = \frac{1}{c} \int_S (4\pi\mathbf{j} + \frac{\partial \mathbf{D}}{\partial t}) \cdot \mathbf{n} da, \quad (\text{A.8})$$

$$\oint_C \mathbf{E} \cdot d\mathbf{l} = -\frac{1}{c} \int_S \frac{\partial \mathbf{B}}{\partial t} \cdot \mathbf{n} da. \quad (\text{A.9})$$

Similar to the procedure above this leads to

$$\mathbf{n} \times (\mathbf{H}_2 - \mathbf{H}_1) = \mathbf{j}, \quad (\text{A.10})$$

$$\mathbf{n} \times (\mathbf{E}_2 - \mathbf{E}_1) = 0. \quad (\text{A.11})$$

Since we do our calculations by means of potentials we rewrite the equations to get conditions for potentials instead of fields. In homogeneous media, $\mathbf{D} = \epsilon \mathbf{E}$,

A. Calculations

equation (A.6) can be rewritten as

$$\epsilon_1 \frac{\partial \phi_1}{\partial n} - \epsilon_2 \frac{\partial \phi_2}{\partial n} = 4\pi\sigma \quad (\text{A.12})$$

where $\partial/\partial n$ is the derivative in the direction normal to the surface.

From the continuity of the tangential electric field (A.11) we get for the potential

$$(\nabla \phi_1)^\parallel = (\nabla \phi_2)^\parallel \quad (\text{A.13})$$

A.2. Potentials in media

If we look at a system with free charges ρ_f and bound charges ρ_b we can introduce two different potentials

$$\nabla^2 \phi_0 = -4\pi\rho_f, \quad (\text{A.14})$$

$$\nabla^2 \phi = -4\pi(\rho_f + \rho_b). \quad (\text{A.15})$$

These correspond to the electric displacement and the electric field

$$\mathbf{D} = -\nabla \phi_0, \quad (\text{A.16})$$

$$\mathbf{E} = -\nabla \phi. \quad (\text{A.17})$$

In a homogeneous medium we can use the proportionality of these fields, $\mathbf{D} = \epsilon \mathbf{E}$, to introduce an additional differential operator

$$\begin{aligned} \nabla^2 \phi_0 &= -\nabla \mathbf{D} = -\nabla \epsilon \mathbf{E} = \nabla \epsilon \nabla \phi = -4\pi\rho_f, \\ \nabla \cdot \epsilon \nabla &= \epsilon \nabla^2 + (\nabla \epsilon) \cdot \nabla = \epsilon(\nabla^2 + e). \end{aligned}$$

A. Calculations

Therefore the new operator is defined as

$$e = \frac{1}{\epsilon}(\nabla\epsilon) \cdot \nabla. \quad (\text{A.18})$$

With the help of this operator we can deduce the free charge density directly from the potential ϕ

$$(\nabla^2 + e)\phi = -4\pi\frac{\rho_f}{\epsilon}. \quad (\text{A.19})$$

The Green's functions for the differential operators have to fulfill

$$\nabla^2 G_0 = -4\pi\delta(\mathbf{r} - \mathbf{r}'), \quad (\text{A.20})$$

$$(\nabla^2 + e)G = -4\pi\delta(\mathbf{r} - \mathbf{r}'), \quad (\text{A.21})$$

where G_0 is the electrostatic Green's function for unbound media that we already encountered in section 2.1.3, G is a Green's function that incorporates the geometry of the system and in general has no simple analytic form. If we combine the two equations above we can get

$$(\nabla^2 + e)(G - G_0) = eG_0. \quad (\text{A.22})$$

Since G is the Green's function to the occurring differential operator the solution is

$$G - G_0 = \frac{1}{4\pi}GeG_0 = \frac{1}{4\pi}G_0eG, \quad (\text{A.23})$$

where the second equality is obtained by an iterative solution to this Dyson like equation.

We can express ϕ through the Green's function for (A.19) and get

$$\nabla^2\phi = -4\pi\frac{\rho_f}{\epsilon} - e\phi = -4\pi\frac{\rho_f}{\epsilon} - eG\frac{\rho_f}{\epsilon}. \quad (\text{A.24})$$

A. Calculations

Inserting equation (A.14) on the left side gives

$$-4\pi(\rho_f + \rho_b) = -4\pi\frac{\rho_f}{\epsilon} - eG\frac{\rho_f}{\epsilon}. \quad (\text{A.25})$$

We multiply this equation with G_0 from the left and use (A.23) to get

$$G_0\rho_b = G_0\left(\frac{1}{\epsilon} - 1\right)\rho_f + (G - G_0)\frac{\rho_f}{\epsilon} = \left(\frac{G}{\epsilon} - G_0\right)\rho_f. \quad (\text{A.26})$$

A.3. Exciton wave functions

To calculate the exciton wave functions, which we need for the calculation of the optical response, we use products of the single particle wave functions ϕ_i of electron and hole, $i = e, h$, which satisfy the Schrödinger equation

$$H_0\phi_\mu^i = \left(-\frac{1}{2}\nabla_i^2 + U_{conf}^i\right)\phi_\mu^i = \varepsilon_\mu^i\phi_\mu^i. \quad (\text{A.27})$$

The exciton wave functions then are

$$\psi(\mathbf{r}_e, \mathbf{r}_h) = \sum_{\mu\nu} c_{\mu\nu}\psi_{\mu\nu}(\mathbf{r}_e, \mathbf{r}_h) = \sum_{\mu\nu} c_{\mu\nu}\phi_\mu^e(\mathbf{r}_e)\phi_\nu^h(\mathbf{r}_h). \quad (\text{A.28})$$

Now we can set up the following Schrödinger equation

$$\left(-\frac{1}{2}\nabla_e^2 - \frac{1}{2}\nabla_h^2 + U_{conf}^e(\mathbf{r}_e) + U_{conf}^h(\mathbf{r}_h) - G(\mathbf{r}_e, \mathbf{r}_h)\right)\psi = E\psi, \quad (\text{A.29})$$

where G is the Greens function of the Coulomb interaction. It can be split into three parts,

$$G(\mathbf{r}_e, \mathbf{r}_h) = G^0(\mathbf{r}_e, \mathbf{r}_h) + G^{ind}(\mathbf{r}_e, \mathbf{r}_h) + \Sigma(\mathbf{r}_e, \mathbf{r}_h). \quad (\text{A.30})$$

The direct interaction $G^0(\mathbf{r}, \mathbf{r}') = 1/\epsilon|\mathbf{r} - \mathbf{r}'|$, the indirect Coulomb interaction through induced charges G_{ind} and Σ , the self interaction of the electron/hole via

A. Calculations

the environment. Here the latter two depend on the geometry of the system. With the density matrix $\rho_{\mu\mu'}^i = \phi_\mu^{i\dagger}\phi_{\mu'}^i$, the representations of these operators in our basis can be written as

$$\begin{aligned}\langle\mu\nu|G^0|\mu'\nu'\rangle &= \int \rho_{\mu\mu'}^e(\mathbf{r}_e) \frac{1}{\epsilon|\mathbf{r}_e - \mathbf{r}'_h|} \rho_{\nu\nu'}^h(\mathbf{r}_h) d\tau_e d\tau_h \\ \langle\mu\nu|G^{ind}|\mu'\nu'\rangle &= \int \rho_{\mu\mu'}^e(\mathbf{r}_e) G^{ind}(\mathbf{r}_e, \mathbf{r}_h) \rho_{\nu\nu'}^h(\mathbf{r}_h) d\tau d\tau' \\ \langle\mu\nu|\Sigma|\mu'\nu'\rangle &= \frac{1}{2} \int \bar{\phi}_\mu^e(\mathbf{r}_e) G^{ind}(\mathbf{r}_e, \mathbf{r}_e) \phi_\mu^e(\mathbf{r}_e) d\tau_e \cdot \delta_{\nu\nu'} \\ &\quad + \delta_{\mu\mu'} \cdot \frac{1}{2} \int \bar{\phi}_\mu^h(\mathbf{r}_h) G^{ind}(\mathbf{r}_h, \mathbf{r}_h) \phi_\mu^h(\mathbf{r}_h) d\tau_h,\end{aligned}$$

where the one-half factor in the last equation follows from the adiabatic building of the charge distribution [7].

Now we have all ingredients to construct the Hamiltonian in the single particle basis. By diagonalizing it, we get the energy states and coefficients in (A.28) for the excitonic wave functions of the complete system.

B. Conventions and Conversions

B.1. Atomic Units

Atomic units build a unit system that is based only on natural constants, it is therefore called a natural unit system. The values of the four following constants are set to unity by definition:

dimension	symbol	name	SI – units
mass	m_e	rest mass of electron	$9.109 \cdot 10^{-31} kg$
charge	e	elementary charge	$1.602 \cdot 10^{-19} C$
electric constant	$1/(4\pi\epsilon_0)$	Coulomb force constant	$8.987 \cdot 10^9 VmC^{-1}$
angular momentum	\hbar	reduced Planck constant	$1.054 \cdot 10^{-34} Js$

From these definitions we can derive the units for all other dimensions, the most important are:

dimension	symbol	name	SI – units
energy	E_h	Hartree Energy	$4.359 \cdot 10^{-18} J$
length	a_0	Bohr radius	$5.291 \cdot 10^{-11} m$
time			$2.418 \cdot 10^{-17} s$

The advantage of atomic units is simplicity of equations, e.g. the Hamiltonian of a hydrogen atom:

$$H_{SI} = -\frac{\hbar}{2m_e} \nabla^2 - \frac{e^2}{4\pi\epsilon_0 r} \longrightarrow H_A = -\frac{1}{2} \nabla^2 - \frac{1}{r} \quad (\text{B.1})$$

B.2. Gaussian-CGS Units

Although the units of the electric field are pinned down in the atomic unit system we have to introduce additional definitions to fix the units for magnetism. There are two common variants of atomic units the SI and the Gauss-CGS systems. Since many theoretical calculations are more convenient in CGS and some physical facts are more inherent we used these in this thesis.

In the following table we show a comparison of Maxwell's equations in SI and Gaussian-CGS units:

name	Gaussian	SI
Gauss's law	$\nabla \cdot \mathbf{E} = 4\pi\rho$	$\nabla \cdot \mathbf{E} = \frac{\rho}{\epsilon_0}$
Gauss for magnetism	$\nabla \cdot \mathbf{B} = 0$	$\nabla \cdot \mathbf{B} = 0$
Faraday's law	$\nabla \times \mathbf{E} = -\frac{1}{c} \frac{\partial \mathbf{B}}{\partial t}$	$\nabla \times \mathbf{E} = -\frac{\partial \mathbf{B}}{\partial t}$
Ampere's law	$\nabla \times \mathbf{B} = \frac{4\pi}{c} \mathbf{j} + \frac{1}{c} \frac{\partial \mathbf{E}}{\partial t}$	$\nabla \times \mathbf{B} = \mu_0 \mathbf{j} + \frac{1}{c^2} \frac{\partial \mathbf{E}}{\partial t}$

B.3. Energy conversion

We use vacuum wavelength as measure for the energy of incoming light. Though strictly it has the wrong dimension it can be definitely mapped to a certain energy. Usually in this context eV is the unit of choice but is much less descriptive. Therefore we will give you the relation between these units.

The energy of an electromagnetic wave is given by

$$E_\gamma = \hbar\omega = \hbar 2\pi\nu = \hbar 2\pi \frac{c}{\lambda}, \quad (\text{B.2})$$

where c and λ are the speed of light and the light wavelength in vacuum. The values for the occurring constants are [25]

$$\begin{aligned} \hbar &= 6.58211899 \times 10^{-16} \text{eV s}, \\ c &= 2.99792458 \times 10^{17} \text{nm/s}. \end{aligned}$$

B. Conventions and Conversions

The conversion from vacuum wavelength to eV is therefore

$$E[\text{eV}] = \frac{1239.84}{\lambda[\text{nm}]}.$$
 (B.3)

Since we used Hartree units for many of our calculations we will additionally note the relation between eV and E_h

$$E[E_h] = 27.211385 \cdot E[\text{eV}].$$

Bibliography

- [1] Ulrich Hohenester and Andreas Trügler. Mnpbem - a matlab toolbox for the simulation of plasmonic nanoparticles. *Computer Physics Communications*, 183(2):370–381, 2012.
- [2] F. J. García de Abajo and A. Howie. Retarded field calculation of electron energy loss in inhomogeneous dielectrics. *Phys. Rev. B*, 65:115418, Mar 2002.
- [3] Harry A. Atwater. The promise of plasmonics. *SIGDA Newsl.*, 37(9):1:1–1:1, May 2007.
- [4] John David Jackson. *Classical Electrodynamics*. Wiley, 1998.
- [5] D.J. Griffiths. *Introduction to electrodynamics*. Prentice Hall, 1999.
- [6] Charles Coulomb. Premier mémoire sur l'électricité et le magnétisme. *Histoire de l'Academie royale des sciences*, pages 569–577, 1785.
- [7] L. Hedin and S. Lundqvist. Effects of electron-electron and electron-phonon interactions on the one-electron states of solids. *Solid State Physics*, 23:1–181, 1969.
- [8] James Clerk Maxwell. A dynamical theory of the electromagnetic field. *Philosophical Transactions of the Royal Society of London*, 155:459–513, 1865.
- [9] Ulrich Hohenester and Joachim Krenn. Surface plasmon resonances of single and coupled metallic nanoparticles: A boundary integral method approach. *Phys. Rev. B*, 72:195429, Nov 2005.
- [10] L. Novotny and B. Hecht. *Principles of Nano-Optics*. Cambridge University Press, 2006.
- [11] S.A. Maier. *Plasmonics: Fundamentals and Applications*. Springer, 2007.

Bibliography

- [12] E.D. Palik. *Handbook of Optical Constants of Solids Five-volume Set: Handbook of optical constants of solids I, II, & III*. Handbook of Optical Constants of Solids Five-volume Set. Academic Press, 1998.
- [13] Andreas Trügler. *Optical properties of metallic nanoparticles*. PhD thesis, Karl-Franzens Universität Graz, July 2011.
- [14] E. Kretschmann and H. Raether. Radiative decay of nonradiative surface plasmons excited by light. *Z. Naturforsch. A*, 23:2135, 1968.
- [15] Andreas Otto. Excitation of nonradiative surface plasma waves in silver by the method of frustrated total reflection. *Zeitschrift für Physik*, 216:398–410, 1968.
- [16] H. Haug and S.W. Koch. *Quantum Theory of the Optical and Electronic Properties of Semiconductors*. World Scientific, 2004.
- [17] K. Hess. *Advanced theory of semiconductor devices*. IEEE Press, 2000.
- [18] Marlan O. Scully and M. Suhail Zubairy. *Quantum Optics*. Cambridge University Press, 2001.
- [19] H.C. Van De Hulst. *Light scattering: by small particles*. Structure of Matter Series. Dover Publications, 1957.
- [20] V. M. Axt and S. Mukamel. Nonlinear optics of semiconductor and molecular nanostructures; a common perspective. *Rev. Mod. Phys.*, 70:145–174, Jan 1998.
- [21] L.H. Ryder. *Quantum Field Theory*. Cambridge University Press, 1996.
- [22] Viktor Myroshnychenko, Jessica Rodriguez-Fernandez, Isabel Pastoriza-Santos, Alison M. Funston, Carolina Novo, Paul Mulvaney, Luis M. Liz-Marzan, and F. Javier Garcia de Abajo. Modelling the optical response of gold nanoparticles. *Chem. Soc. Rev.*, 37:1792–1805, 2008.
- [23] Gustav Mie. Beiträge zur optik trüber medien, speziell kolloidaler metallösungen. *Annalen der Physik*, 330(3):377–445, 1908.

Bibliography

- [24] Ehud Shaviv, Olaf Schubert, Marcelo Alves-Santos, Guido Goldoni, Rosa Di Felice, Fabrice Vallee, Natalia Del Fatti, Uri Banin, and Carsten Sönnichsen. Absorption properties of metal-semiconductor hybrid nanoparticles. *ACS Nano*, 5(6):4712–4719, 2011.
- [25] Peter J. Mohr, Barry N. Taylor, and David B. Newell. Codata recommended values of the fundamental physical constants: 2006. *Rev. Mod. Phys.*, 80:633, 2008.